Development of Microglia sufficient Vascularized Brain Organoids to study three-way Neuro-Immune-Vascular Interactions

A Thesis submitted to

Indian Institute of Science Education and Research Pune in partial fulfilment of the requirements for the BS-MS Dual Degree Programme

by

Mihir Shridhar Dingankar

Indian Institute of Science Education and Research Pune

Dr. Homi Bhabha Road,

Pashan, Pune 411008, INDIA.

Date: 1st April, 2023

Under the guidance of

Supervisor: Dr. Florent Ginhoux and Dr. Satish Kumar Tiwari

Singapore Immunology Network, A*STAR

From May 2022 to Mar 2023

INDIAN INSTITUTE OF SCIENCE EDUCATION AND RESEARCH PUNE

Certificate

This is to certify that this dissertation entitled **Development of Microglia sufficient Vascularized Brain Organoids to study three-way Neuro-Immune-Vascular Interactions** towards the partial fulfilment of the BS-MS dual degree programme at the Indian Institute of Science Education and Research, Pune represents work carried out by Mihir Shridhar Dingankar at the Singapore Immunology Network, A*STAR under the supervision of Dr. Florent Ginhoux and Dr. Satish Kumar Tiwari (Singapore Immunology Network) during the academic year 2022-2023.

Dr. Florent Ginhoux

Senior Principal Investigator

Singapore Immunology Network

Dr. Satish Kumar Tiwari

Research Fellow, Laboratory of Dr. Florent Ginhoux

Singapore Immunology Network

Committee:

Supervisor: Dr. Florent Ginhoux, Singapore Immunology Network, A*STAR

Co-supervisor: Dr. Satish Kumar Tiwari, Singapore Immunology Network, A*STAR

TAC Member: Prof. Satyajit Rath, Department of Biology, IISER Pune

Declaration

I hereby declare that the matter embodied in the report entitled **Development of Microglia sufficient Vascularized Brain Organoids to study three-way Neuro-Immune-Vascular Interactions** are the results of the work carried out by me at the Singapore Immunology Network, A*STAR, under the supervision of Dr. Florent Ginhoux and Dr. Satish Kumar Tiwari and the same has not been submitted elsewhere for any other degree

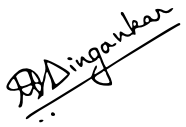

Mihir Shridhar Dingankar

Date: 1st April, 2023

Table of Contents

Certificate **2**
Declaration **3**
List of Tables **6**
List of Figures **7**
Abstract **8**
Acknowledgements **9**
Contributions **10**
1. Introduction **11**
1.1 The exclusivity of human neurodevelopment 13
1.2 One model to rule them all: An emphasis on human 15
1.2.1 Human (Induced) Pluripotent Stem Cells (hiPSC) 17
1.2.2 “Induced” Pluripotent Stem Cells 17
1.2.3 Organoids and Embryoid Bodies 19
1.2.4 iPSC-derived Brain Organoids 19
1.2.5 Limitations of the Brain Organoid Model 21
1.3 Microglia 22
1.3.1 Developmental and Pathogenic Roles of Microglia 24
1.3.2 iPSC-derived Microglia - iMicros 26
1.4 iPSC-derived Blood Vessels and the idea behind this Project 29
2. Materials and Methods **32**
2.1 Materials and Reagents: 32
2.2 Media composition 34
2.3 Methods 37
2.3.1 Human iPSC culture and maintenance 37
2.3.2 Induced (iPSC-derived) Primitive Macrophage (iMac) Differentiation 38
2.3.3 Brain organoid differentiation: Lancaster and DS 39
2.3.4 Blood Vessel Organoid Protocol Development - All Protocols 41
2.3.5 Protocol for the generation of Blood Vessel Organoids 43
2.3.6 Fusion of Brain and Blood Vessel Organoids 45
2.3.7 Co-culture of Brain/ Fused vascularized brain organoids with iPSC-derived primitive macrophages 45
2.3.8 Organoid Fixation and Sectioning 46
2.3.9 Immunohistochemistry sample preparation 46
2.3.10 Flow cytometry sample preparation 46
3. Results **47**
3.1 Human iPSC maintenance and ensuring colony health 47
3.2 iPSC-derived brain organoids 48
3.3 iPSC-derived Microglia 52
3.4 hiPSC-derived Blood Vessel Organoids 55
3.5 Fusion Vascularized Brain Organoids 59
3.6 Co-culture of Fusion organoids with iPSC-derived Primitive Macrophages 64

4. Discussion.....70
4.1 Generation and co-culture of hiPSC-derived Brain Organoids.....71
4.2 iPSC-derived Blood Vessel Organoids (BVOs).....71
4.3 Development of a Protocol for the Vascularization of Brain Organoids.....73
4,4 The developmental role of Microglia and future directions.....73
4.5 Limitations.....75
5. References.....76

List of Tables

Table 1: Comparison of the different endothelial cell/blood vessel organoid generation protocols in literature

List of Figures

Fig. 1.1: Schematic displaying the Symmetric and Asymmetric divisions which occur during neurogenesis.
Fig. 1.2: Schematic displaying the organization of Progenitor layers during Neurogenesis.
Fig. 1.3: Schematic displaying the Isolation of hES cells and generation of hiPS cells.
Fig. 1.4: Comparisons of the protocols used to generate iPSC/ESC-derived microglia.
Fig. 3.1: Morphological identification of iPSC colony health and identification of areas of differentiation.
Fig. 3.2: Differentiation of hiPSCs into Brain Organoids.
Fig. 3.3: Gating strategy for identification of the different CNS cell types seen in the developing brain organoid at 44 days after seeding.
Fig. 3.4: Observation of Neuronal Synapses in Day 44 Brain Organoids.
Fig. 3.5: Differentiation of hiPSCs into Brain Organoids using Dual-SMAD inhibition.
Fig. 3.6: Induced Macrophage (iMac) differentiation of human iPSCs.
Fig. 3.7: Induced Macrophage (iMac) confirmation using Flow Cytometry.
Fig. 3.8: Representative schematic and gating strategy for protocols reported in the literature for the generation of iPSC-derived endothelial cells or blood vessels.
Fig. 3.9: Generation of hiPSC-derived Blood Vessel Organoids using our optimized protocol.
Fig. 3.10: Morphological features seen in the Blood vessel organoids.
Fig. 3.11: Gating strategy for identification of CD31+ endothelial cells.
Fig. 3.12: Fusion of iPSC-derived blood vessel and brain organoids and the generation of fused vascularized brain organoids.
Fig. 3.13: Immunohistochemistry images of fixed and frozen 18um cryosections of fused vascularized brain organoids
Fig. 3.14: Co-culture of Fusion Vascularized Brain Organoids with iPSC-derived primitive macrophages
Fig. 3.15: Gating strategy for co-cultured Brain Organoids
Fig. 3.16: Gating strategy for co-cultured Fusion Vascularized Brain Organoids

Abstract

Most of our understanding of human embryonic development is limited by technical and ethical difficulties in acquiring samples and mainly relies on comparative studies in mice and other higher mammals. Although this approach works for very early developmental events, soon fundamental evolutionary differences begin to add a layer of complexity which simply does not exist in mice. Recently, human induced pluripotent stem cells (hiPSC) or human embryonic stem cell (hESC) based organoids have emerged as a strong model to recapitulate essential aspects of human development *in vitro*. The developing human brain, unquestionably the crowing achievement of evolution, is the most difficult to study in mice due to significant species-specific differences necessitating a model able to recapitulate cellular diversity and organizational features during human development *in vitro*. In this work, we build on the complexity of brain organoids by introducing a vascular network as well as the microglial resident immune compartment. In these immune-sufficient vascularized organoids, we observe a close apposition of blood vessels with neural progenitors and neurons. This emphasises the strength of our model for future explorations of vascular involvement in neurodevelopment. Incorporation of the microglial compartment affects not only the neurodevelopmental processes but appears to show a trending increase in the proportion of endothelial cells giving a closer insight into the early vascularisation of the human brain. Overall, the development of this model provides a unique platform for further transcriptomic characterization of microglial heterogeneity and contributes to the long-term goal of incorporating a perfusable circulatory network into organoids.

Acknowledgements

All good things must come to an end before something even better can begin. This is what I have been telling myself to help me get through these last few months in Singapore. It never is just about the science or the research, that's just an excuse to meet amazing new people. People who understand what you're going through and people who listen to you when you need someone to talk to and keep talking even after you've run out of things to say. It's the people who don't care that they didn't know you a month ago but make you feel like they did. It's the people who jump just as high as you every time you celebrate while being more than willing to board a sinking ship during the slightest of storms. I wouldn't be exaggerating, if I said THIS is why I love doing science. It is this emotion that I am finally letting myself experience now that my time in the FG Lab is about to come to a close.

To Satish, you have seen me grow from the day I got couldn't find my way to lab to today when I really don't want to find my way out of it. Thank you for standing by me when my iPSCs didn't and brain organoids looked like something out of the Alien movies. Through the (astonishing) collection of mistakes I made almost daily to my wildest ideas about what could've gone wrong, you were the most patient mentor I could've asked for. I always knew that even when my cells couldn't take it anymore, you could. To Dr. Ginhoux, thank you for always ending every discussion of a failed experiment with, "Well good! At least we now know it doesn't work.". Your brilliance and ability to put narrowly construed research questions into perspective in literally unmatched. Personally, however, thank you for always asking me how things were going. All through the graduate school application process, despite your extremely demanding schedule, you always found time for me. It is not often that a singular experience has such a butterfly effect on the future, but for my increased fascination with immunology and my ability to ask exciting questions I cannot thank you enough Dr. Ginhoux and Satish. To Victor and his fiancée, you showed me some of the best food (and the stinkiest fruits) in Singapore. Thank you for helping tick many items off my bucket list. To William, thank you for always finding me while I was having lunch. I really enjoyed those chats. To Kat, I don't know what to say but just that I always reached peak happiness after I talked to you. Your sheer joy at my achievements and our discussion of immunology and grad school made every day feel a lot brighter. To Chris, I

am going to miss the weird questions you asked while I was working in the lab and the very politically incorrect discussions. And lastly, Ying Xiu, thank you for always checking up on me while I was working and for taking me around to eat new local food. On the list of people I am going to miss the most, you're quite near the top.

As this will be the end of my time at IISER, Pune, my emotions are getting the better of me, but what gives me the most respite is that the best of friends I made will accompany me the US for grad school. Case in point - Shivani, not mincing my words, I couldn't have done this without you. You talked to me every single time I was upset or anxious or overthinking…the list continues. Now I haven't conducted any double-blind studies, but after every call, I was sure things would be alright. It really takes some effort to get me to stop talking but you always could and for that, I just say thank you.

I cannot end this without talking about someone without whom I never would have come to Singapore. Satyajit, you conduct the most fascinating Immunology courses. My interest in immunology started because of you (are you to blame?!?). You gave me direction when I was trying to decide how to approach research in immunology and your advice helped me find the Singapore Immunology Network and Dr. Ginhoux. So I begin this project as it started, thank you so much Dr. Ginhoux and Dr. Rath for replying to my email.

Contributions

Contributor name	Contributor role
Dr. Florent Ginhoux, Dr. Satish Kumar Tiwari	Conceptualization Ideas
Dr. Florent Ginhoux, Dr. Satish Kumar Tiwari, Mihir Dingankar	Methodology
-	Software
Mihir Shridhar Dingankar	Validation
Mihir Shridhar Dingankar	Formal analysis
Mihir Shridhar Dingankar, Dr. Satish Kumar Tiwari	Investigation
Singapore Immunology Network	Resources
-	Data Curation
Mihir Shridhar Dingankar	Writing - original draft preparation
Dr. Satish Kumar Tiwari	Writing - review and editing
Mihir Shridhar Dingankar	Visualization
Dr. Florent Ginhoux, Dr. Satish Kumar Tiwari	Supervision
Dr. Florent Ginhoux, Dr. Satish Kumar Tiwari	Project administration
Dr. Florent Ginhoux	Funding acquisition

1. Introduction

Neurogenesis, defined most broadly, is the process by which neurons are formed from neural stem cells and their derivative progenitors during the development of the mammalian CNS (Götz and Huttner, 2005). The inherent increase in complexity of human brain organization from other higher mammals poses a very fundamental question in biology: How is neurogenesis in particular and neurodevelopment, in general, different across species and more specifically in humans? Basically, the source of our increased cognitive and emotional functions and the answer to the question of what makes us, us

Before a comprehensive discussion of the project as well as the model system designed in the project, it is instructive to look at an overview of mammalian neurodevelopment. In this section, I will primarily focus on the description of the developing cerebral cortex, given its importance in higher human motor and cognitive functions (Geschwind and Rakic, 2013; Silva *et al.*, 2019). The cerebral cortex develops from an invagination and expansion at the anterior end of the neural tube (Andrews *et al.*, 2022). The single-cell layer of the neural tube gives rise to all the neuronal and glial cell subtypes which populate the cerebral cortex. Just as importantly, the polarity and radial organization of this founding population define the architecture throughout development and adulthood (Andrews *et al.*, 2022).

The emergence of diversity and complexity of neuronal and glial subtypes is primarily the result of two kinds of cell divisions: Symmetric Proliferative divisions and Asymmetric Neurogenic divisions (Götz and Huttner, 2005). Early during development - in the first trimester in humans and before Embryonic Day (E) 9/10 in mice - most of the divisions are proliferative - increasing the precursor pool (keep a look out for its implications in the next section) (Andrews *et al.*, 2022). In these stages, the developing cortex is populated by cells of the neural tube called neuroepithelial cells. These cells show characteristics of classical epithelial cells and are polarized along the apical-basal axis (Götz and Huttner, 2005) with projections extending all the way from the apical zone at the ventricular surface to the basal region (Andrews *et al.*, 2022). It is at this stage that we come across a characteristic feature exhibited by early neural precursor cells called inter-kinetic nuclear migration (IKNM) (Takahashi *et al.*, 1993). The nuclei of

neuroepithelial cells shuttle between the ventricular surface during the G1 phase and then to the basal surface during the S phase and back to the ventricular surface during the G2 phase (Kosodo *et al.*, 2011).

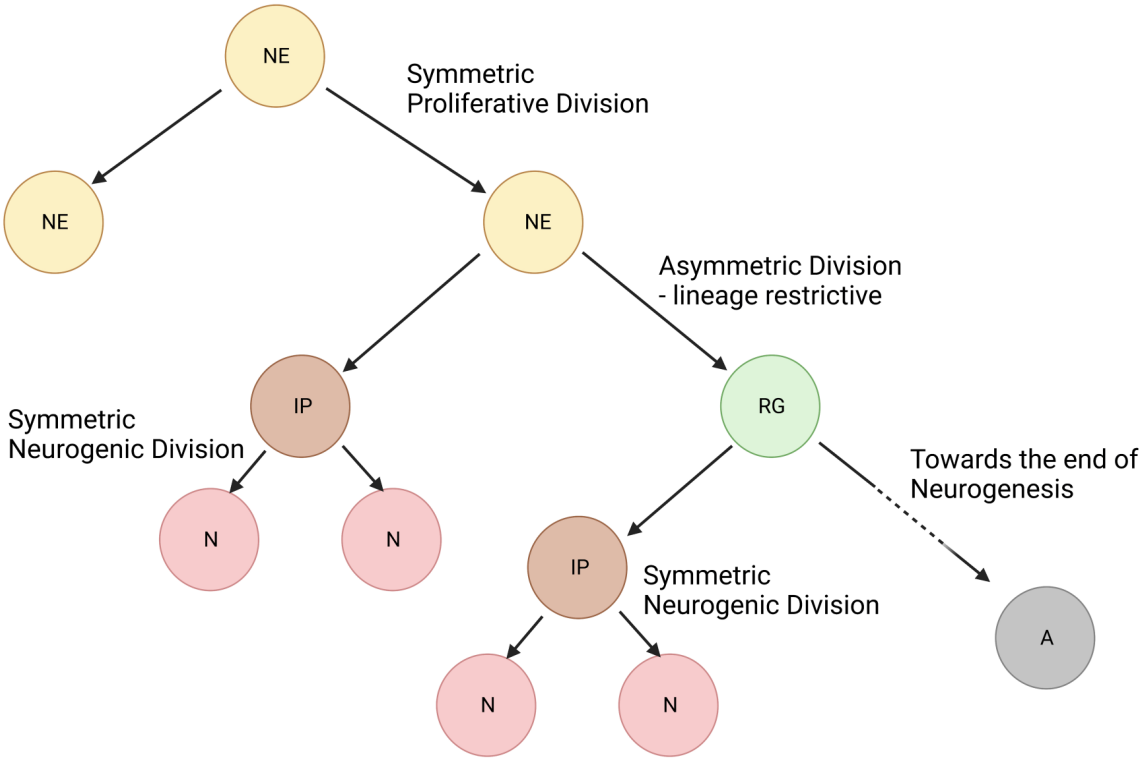

Fig. 1.1: Schematic displaying the Symmetric and Asymmetric divisions which occur during neurogenesis: The Neuroepithelial (NE) cells can undergo proliferative or asymmetric divisions with the latter giving rise to Radial Glia (RGs). These RGs can, in turn, proliferate or differentiate into Neurons (N) as well as transit-amplifying cells called Intermediate (Basal) Progenitors (IP). Towards the end of neurogenesis, the RGs mature into Astrocytes (A). Diagram based on Götz and Hunter, 2005 (Götz and Huttner, 2005)

At the onset of neurogenesis, typically at the end of the first trimester in humans and around E12/13 in mice, the neuroepithelial cells transform into a more lineage-restricted progenitor population via an asymmetric division (Götz and Huttner, 2005; Andrews *et al.*, 2022). While the neuroepithelial cells are rarely lineage-restricted, the newly emerging radial glia (only ventricular Radial glia - vRG at this stage) can mostly give rise to a single lineage of cells. Most of the neurons in the CNS emerge from Radial glial progenitors (Anthony *et al.*, 2004) when radial glia undergo asymmetric divisions giving rise to a radial glial cell as well a neuron. An essential attribute of the ventricular radial

glia at this stage is their persistent basal process, which is thought to guide neuronal migration away from the ventricular zone (Rakic, 2003; Subramanian *et al.*, 2017).

It is important, at this stage, to notice a pattern here. Neurogenesis often proceeds through a common repeating motif of symmetric proliferative division accompanied by asymmetric neurogenic divisions. This provides an interesting avenue for variation between species. A small increase in the number of proliferative divisions can give rise to a spectacular increase in the final number of neurons generated (Rakic, 2009). Using the language of the description above: more divisions in the neuroepithelial cells give rise to an exponentially higher number of vRG cells and thus result in an exponentially higher final number of neurons.

1.1 The exclusivity of human neurodevelopment

The mammalian cortex is a layered sheet consisting of six layers of neurons which emerge during development in a bottom-up manner. This generalization, however, does not by any means lessen the sheer increase in complexity seen in the human cortex. With variabilities in this structure seen corresponding to the function of each location, the human brain exhibits more than 50 such distinct cytoarchitectural areas (Rakic, 2003). This complexity is further emphasised by the organization of the progenitor zones. In the developing rodent brain, the progenitor zones can be broadly divided between a ventricular zone (VZ) and an outer subventricular zone (SVZ) (this describes a subset and not a complete list of the progenitor zones). The primary proliferative zone is the ventricular zone populated by the Radial Glia (RG). These RGs can undergo symmetric proliferative divisions as well asymmetric divisions to generate neurons or a transit-amplifying population called the Basal Progenitors (BP). These BPs migrate outwards to the subventricular zones and divide symmetrically at most a couple of times before giving rise to neurons (Hansen *et al.*, 2010; Martynoga *et al.*, 2012). In mice, these RG give rise to a majority of neurons in the cerebral cortex and ultimately end with the generation of astrocytes and oligodendrocytes (Malatesta *et al.*, 2003; Rash *et al.*, 2019; Allen *et al.*, 2022).

In humans, the SVZ is split into an inner SVZ (ISVZ) and a massively expanded outer SVZ (OSVZ), which contributes to the cortical size and complexity. A population of RG-like cells was known to populate this region. Their characteristics, however, would remain elusive for a long period of time. It was the work from Hansen, D. et al. that first managed to study this elusive population of cells. True to their name these “outer” Radial Glia (oRG) expressed glial markers like GFAP (glia-fibrillary acidic protein), but unlike their ventricular counterparts, only extended a basal projection to the pial surface (Hansen *et al.*, 2010). These cells also underwent proliferative as well as horizontal asymmetric divisions. In the latter circumstance, the cell which inherited the basal process remained an oRG cell whereas the other daughter cell often proliferated one or more times before acquiring markers of excitatory or inhibitory neuronal commitment (formation of both oRG daughter cells after horizontal divisions also occurs in rare cases) (Hansen *et al.*, 2010). A curious feature of these cells was a basal translocation of the entire soma immediately prior to cytokinesis (Hansen *et al.*, 2010; Ostrem *et al.*, 2014). This progressive basal movement is thought to be essential for the expansion of the OSVZ as neurogenesis progresses.

Temporally, the ventricular zone is the dominant progenitor zone in humans before Gestational Week (GW) 11.5 where it resembles the corresponding zone during early mouse neurogenesis. By GW 15.5, however, a lot has changed and now, the OSVZ is the dominant progenitor zone representing more than 75% of all the proliferation (Hansen *et al.*, 2010).

The purpose of this primer on neurogenesis is three-fold. Firstly, it highlights the important steps and features of human neurogenesis which will be brought up again in the later sections when *in vitro* studies of neurogenesis will be discussed. Secondly, it highlights the three-dimensional nature of neuron formation, and lastly, it emphasises the stark differences seen in mice. The latter emphasises the need for a more “human” model for the study of neurogenesis and neurodevelopmental processes as well as the pitfalls of using mouse models to study human neurodevelopmental disorders.

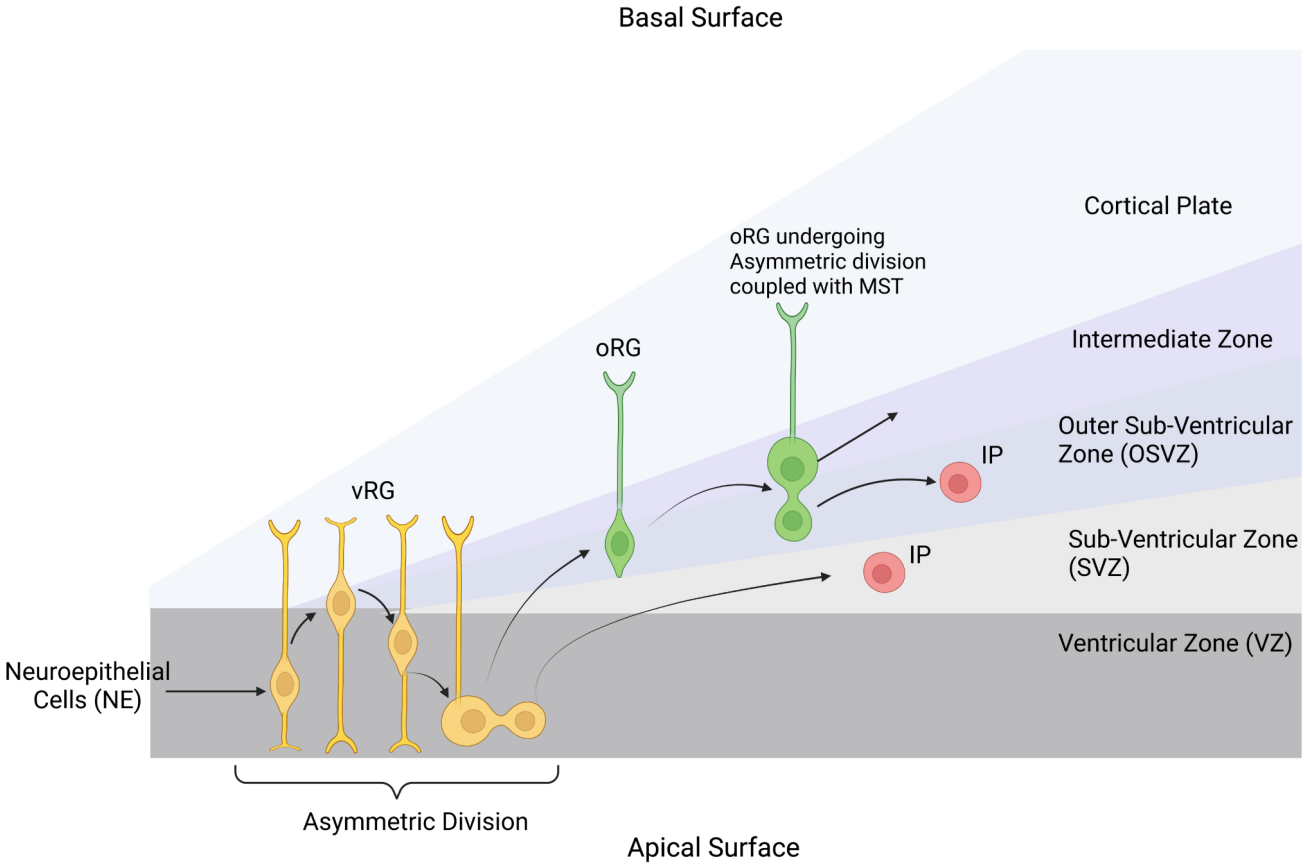

Fig. 1.2: Schematic displaying the organization of Progenitor layers during Neurogenesis: The figure illustrates the diversity and organization of the cell types during neurogenesis. The oRG cells constitute the dominant progenitor group in humans and undergo Mitotic Somal Translocation (MST) which is thought to be responsible for the basal expansion of progenitor zones. The intermediate progenitors (IPs) can proliferate a few times before differentiating into neurons. Schematic based on Andrews, M et al. 2022 (Andrews *et al.*, 2022)

1.2 One model to rule them all: An emphasis on human

What are the characteristics of a good model system to study immunology or neurobiology? Firstly, the model system should recapitulate the human features that are being studied. Secondly, it should yield the correct cells in sufficient numbers to support characterization. Thirdly, it should be amenable to probing, genetic manipulations, as well as imaging.

Based purely on the first qualifier, the most ideal system to study human neurodevelopment would be human brains. However, ethical as well as practical constraints of human embryo research rule this out in most circumstances. Although

mouse models satisfy the two latter constraints, it is increasingly obvious that significant neurodevelopmental differences exist between humans and mice. For example, cell cycle timings in humans, curiously, are almost 4x as long as in mice but the time frame of cortical neurogenesis is almost 20x longer in humans (Geschwind and Rakic, 2013). Furthermore, mice are born at a stage where their brains are developmentally primitive as compared to newborn humans causing differences in the role external stimuli play during neuronal maturation (Geschwind and Rakic, 2013; Sidorov *et al.*, 2020). Of greater interest, however, is the observation that genetic mutants which in humans are associated with microcephaly and lissencephaly (smooth cerebral cortex) as well as neuro infections which lead to microcephaly (eg. the Zika virus infection) do not cause any defects in mice (a slightly humorous interpretation being that the mouse brains were "small" to begin with)(Lancaster *et al.*, 2013; Qian *et al.*, 2016; Marshall and Mason, 2019). Furthermore, owing to the small size of mouse embryonic brains, the study of rare cell populations becomes difficult due to insufficient cell numbers for proper transcriptomic or proteomic characterizations.

Owing to these considerations, an alternative model was needed to study early neurodevelopmental time points in humans. This model should preferably have human cell types and develop at a timescale similar to humans. It should recapitulate features seen *in vivo* and should provide avenues for genetic manipulation. Most importantly, it should display the "correct" three-dimensional organization seen in the developing neuroectoderm. This is where we come across the human Induced Pluripotent Stem Cell (hiPSC)-derived Brain Organoids. Before immersing in a full-fledged discussion on Brain Organoids and recent development in organoid technology, it is interesting to take a look at the cell type which makes these organoids possible.

1.2.1 Human (Induced) Pluripotent Stem Cells (hiPSC)

Until the last decade of the 20th century, the study of human foetal development was primarily based on the study of a small number of sectioned embryos as well as by comparisons with closely related species. This "conclusion by analogy", however, doesn't work when features specific to human evolution have to be studied. A significant leap in this quest was the isolation of human pluripotent stem cells derived from cultured

human blastocysts (Thomson *et al.*, 1998; Zhu and Huangfu, 2013). These Embryonic Stem (ES) cells are derived from totipotent stem cells. They are capable of unlimited, undifferentiated proliferation in culture as well as differentiation into tissues of all three germ layers in the presence of the appropriate cues (Thomson *et al.*, 1998). It is important to note the difference in terminology, these ES cells can give rise to any tissue of the body but cannot generate an entire organism. These cells highly expressed telomerase and did not exhibit replicative crisis even after long-term culture (Thomson *et al.*, 1998).

Although an extremely powerful model system, three primary limitations prevented their widespread use: Firstly, ethical concerns regarding their isolation from IVF-implanted consensual donors. Secondly, the inability to easily study patient-specific developmental defects, and thirdly necessity for co-culture with Mouse Embryonic Fibroblasts (MEFs) to maintain an undifferentiated state (Thomson *et al.*, 1998; Takahashi *et al.*, 2007).

1.2.2 “Induced” Pluripotent Stem Cells

In 2007, the laboratory of Dr. Shinya Yamanaka at Kyoto University published a landmark study on the generation of pluripotent stem cells from terminally differentiated adult human dermal fibroblasts by the retroviral transduction of four transcription factors (Takahashi and Yamanaka, 2006; Takahashi *et al.*, 2007). These four transcription factors, now commonly referred to as Yamanaka factors, comprise Oct3/4, Sox2, c-Myc, and Klf4. This transduction resulted in the appearance of flat hES cell-like colonies within 25 days, albeit at very low efficiency (Takahashi *et al.*, 2007). These cells showed characteristics of human ES cells, including feeder dependence, expression of human ES cell markers, and similar transcriptional and chromatin profiles, as well as long-term exponential growth (Takahashi *et al.*, 2007). The lab also made further progress at generating c-Myc, viral vector, and integration-free iPS cells at higher efficiencies, which are left out for the sake of brevity (Nakagawa *et al.*, 2008; Okita *et al.*, 2008, 2011).

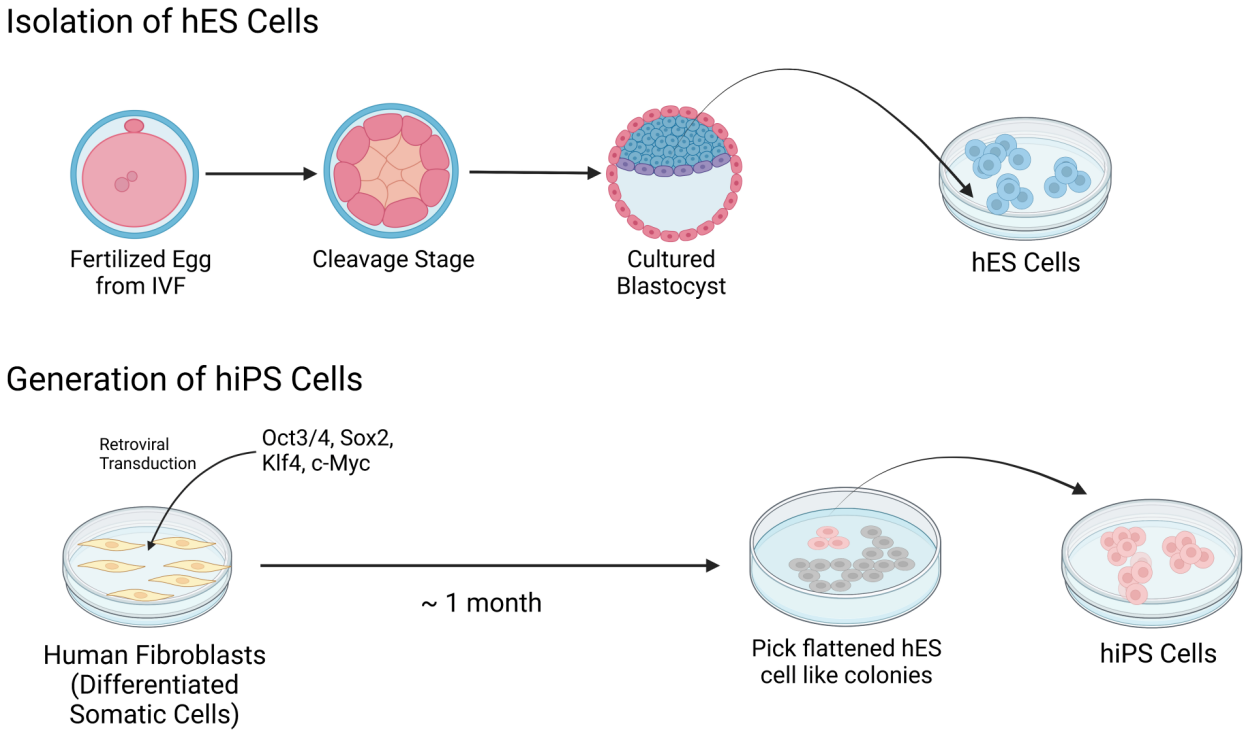

Fig. 1.3: Schematic displaying the Isolation of hES cells and generation of hiPS cells: hES cells are isolated from blastocysts cultured from *in vitro* fertilized eggs. hiPS cells, on the other hand, are generated by retroviral transduction of differentiated somatic cell types. Schematic based on Zhu and Huangfu, 2013 (Zhu and Huangfu, 2013).

This generation of pluripotent stem cells, led to an explosion in the field of stem cell research by greatly minimising the ethical concerns as well as by allowing the development of patient and disease-specific iPS cell lines. These lines could then be used for the study of the normal or aberrant developmental processes and generate large numbers of biologically rare cell types allowing their characterization.

While the generation of biologically relevant cell types from iPS cells is a fascinating problem in itself, an essential aspect of tissue/ organ function is the proper 3D organization of its constituent cell types. This led to the development, in parallel, of a model system which attempts to recapitulate the three-dimensional structure of tissues in addition to their cellular diversity while starting with iPS cells. These so-called iPSC-derived Organoids heralded a giant leap in the study of human development and in the pursuit of personalized medicine.

1.2.3 Organoids and Embryoid Bodies

Embryoid bodies (EBs) form when human ES or iPS cells are grown under conditions of forced aggregation in suspension culture in the absence of LIF (Itskovitz-Eldor *et al.*, 2000). They show spontaneous differentiation into different regions containing cells from all three germ layers. This points to an ability in ES/ iPS cells to regionally self-pattern in the absence of any external patterning cues. However, the generation of any one tissue/organ-specific feature happens at extremely low efficiencies and unpredictably in embryoid bodies. As a result, appropriate growth conditions or developmental cues are often externally provided to direct the differentiation of the embryoid body.

An Organoid is a stem cell-based *in vitro* model which recapitulates many of the organizational features and functional aspects of the corresponding *in vivo* tissue (Zhao *et al.*, 2022). In popular discourse, the terms ‘mini-organs’ or ‘organs in a dish’ are often used. Although these terms have a nice ring to them, they are biologically grossly inaccurate for reasons we will come to in later sections. Instead of devoting the next section on an abstract discussion of organoids, I will focus on Brain organoids while highlighting general organoid concepts.

1.2.4 iPSC-derived Brain Organoids

The differentiation of iPSCs into tissue-specific cell types can typically follow one of two main differentiation strategies: co-culture with a variety of primary or tumour-derived cell types or exposure to defined patterning factors. The first attempts at differentiation of iPSCs into neuronal cell types used the embryoid body approach followed by treatment with high concentrations of Retinoic Acid (RA) (Bain *et al.*, 1995). When these embryoid bodies were plated, a large number of bonafide neuron-like cells were observed. However, spontaneous embryoid body approaches suffer from a large number of contaminating cell types and the use of Retinoic acid was controversial owing to its effect on neuronal subtype specification. The next slate of approaches used two-dimensional culture systems (plates) and utilized co-culture with PA6 cells to induce neuronal differentiation at high efficiencies (Kawasaki *et al.*, 2000). Co-culture

approaches are convenient but limit the subtypes of neurons which can be generated while also suffering from a loss of tractability (Chambers *et al.*, 2009).

What was ideally necessary for successful plate-based approaches was the use of small molecule inhibitors which could direct iPSCs to neurons. Small molecules allow the use of defined conditions which in combination with the use of serum-free media ensures maximal reproducibility when generating neuronal subtypes from ES/iPS cells. An important finding in this direction was that the BMP4 (Bone Morphogenetic Protein-4) inhibited the differentiation of ES cells to neurons in the presence of PA6 cells (Kawasaki *et al.*, 2000). This finding was exploited by the lab of Dr. Lorenz Struder who used inhibition of the BMP signalling pathway using the inhibitor Noggin together with inhibition of the TGF signalling using the inhibitor SB431542 to develop a highly efficient approach for differentiation of ESCs into neurons (Chambers *et al.*, 2009). Both Noggin and SB431542 are inhibitors of SMAD signalling and this approach will be referred to in the later sections as dual-SMAD inhibition.

Around the same time as the development of dual-SMAD inhibition, the study of the natural time course of neurodevelopmental processes in humans. This required a model system which recapitulates the 3D organization and developmental stages of the neuroectoderm at high efficiencies, but which must be free from the use of small molecule inhibition. The solution? A low concentration of FGF-2 (Fibroblast Growth Factor). Embryoid bodies plated in the presence of low FGF-2 in defined media showed the correct organization of neuroepithelial cells into neural rosettes similar to those seen *in vivo* (Zhang *et al.*, 2001; Xia and Zhang, 2009). The next obvious, but challenging, step was to go from the plate to organoids in suspension culture. This challenge was met in a groundbreaking paper from the lab of Dr. Juergen Knoblich where ES/iPS cells were used to develop a brain organoid (Lancaster *et al.*, 2013; Lancaster and Knoblich, 2014). The field-shattering step was the use of Matrigel® (Corning®) a solubilized basement membrane preparation rich in extracellular matrix proteins. After the embryoid bodies were grown in low FGF-2 and subjected to neural induction, they were embedded in a matrigel scaffold (Xia and Zhang, 2009). This matrigel scaffold imposed on the system as “outside to inside” polarization which resulted in exceptional recapitulations of the morphological features seen *in vivo.*

These new brain organoids displayed characteristic features observed during *in vivo* development in humans including adjacent non-overlapping regions expressing discrete forebrain and hindbrain markers reminiscent of an early mid-hindbrain boundary. Over time, further specification of cortical lobes also appeared in the organoids as well as the appearance of other brain regions like the choroid plexus and the retina (Lancaster *et al.*, 2013). In the context of our discussions on neurogenesis, staining for markers of the neuronal developmental stages showed properly organized ventricular and outer Radial Glia with an apical-basal polarization as well as the emergence of intermediate progenitors and excitatory neurons. Furthermore, the neuroepithelia exhibited a pseudostratified morphology and live imaging revealed the presence of interkinetic nuclear migration (IKNM). Moreover, iPSCs derived from patients harbouring microcephaly-inducing mutations showed significantly smaller organoid size as well as a premature oRG to neuron differentiation (Lancaster *et al.*, 2013). I will restrict myself to a description of this subset of similarities. Further readings of the papers written by Dr. Madeline Lancaster on this subject is highly encouraged.

This protocol developed in the lab of Dr. Knoblich has stood the test of time and is used to date with almost no changes. It is also the protocol used in the results and methods section of this work. It was clear at this point that these brain organoids recapitulated certain essential features of human neurodevelopment. It also provided a strong foundation for the development of brain region-specific organoids as well as organoids which highly reproducibly generated cortical features (Qian *et al.*, 2016; Qi *et al.*, 2017; Rosebrock *et al.*, 2022). In classic “cut-paste” fashion, the dual-SMAD inhibition approach was also adapted for use in the brain organoids which has also been used in this work and will be seen in the results as well as in the discussion sections (Sun *et al.*, 2022).

1.2.5 Limitations of the Brain Organoid Model

It is now time to return to my claim that calling organoids “organs in a dish” is inappropriate. Although organoids do recapitulate certain aspects of tissue structure and function, they lack external patterning cues and external signals imposed during fertilization and in the uterus. As a result, the relative spatial location of different brain

regions generated in an organoid can often be jumbled (recent work using so-called “assembloids” made by a fusion of organoids with different brain region specificities has tried to overcome this limitation (Roth *et al.*, 2023). Furthermore, there is significant organoid-to-organoid variability, especially in situations of spontaneous patterning, making it difficult to obtain the large sample sizes necessary for obtaining mechanistic insight (Anand *et al.*, 2023).

The next set of complications with the organoid model arose due to their inherent simplicity. Organoids (at least the simple ones discussed until now, classic foreshadowing) often show a limited number of cell types and lack immune as well as vascular compartments. Given the increasingly appreciated role of immune cells in tissue development and reorganization, the absence of immune cells leads to deviations from *in vivo* development. Furthermore, the absence of a circulatory system leads to necrosis in the core of the organoids where diffusion through the surface does not suffice to ensure nutrient transport (Giandomenico *et al.*, 2021; Sun *et al.*, 2022). This nutrient deprivation in combination with the *in vitro* conditions results in a situation of constant cell stress in the organoid which has been shown to cause defects in the exact recapitulation of the cell subtypes seen *in vivo* (Bhaduri *et al.*, 2020).

Although not all of these problems have a solution and require cautious interpretation of the results seen in the organoids. The simplicity of organoids is a problem which can be further explored. In this work, I attempt to introduce an immune compartment in the brain organoids in the form of microglia while at the same time integrating a vascular compartment comprising endothelial cells and pericytes. I will now move on to a brief description of the microglial and vascular compartments before coming back to a description of the project.

1.3 Microglia

Microglia are the resident macrophages of the central nervous system and have been known to play important roles during brain development and pathophysiology. They emerge in the Yolk Sac (YS) from c-myb independent primitive myeloid progenitors before Embryonic Day (E) 8.0 in mice (typically around E 7.5) giving rise to YS

Macrophages by E 9.0 and with the advent of circulation reaching the developing brain by E 9.5 (Ginhoux *et al.*, 2010; Schulz *et al.*, 2012; Hoeffel and Ginhoux, 2015). The microglia enter through the developing neuroectoderm and are highly proliferative only during embryonic time points (Ginhoux *et al.*, 2010).

A closer look at the ontogeny of microglia reveals the pathways essential for their development. Analysis of the E 8.0 Yolk Sac reveals the presence of three subsets $CD45^{-}$c-kit, $CD45^{+}$c-kit^{-}, and $CD45^{-}$c-kit^{-}. Further analysis at E 9.0 using GFP knock-in on one allele of the Cx3cr1 gene reveals that by E 9.0 two subsets of cells in the YS described as $CD45^{+}$c-kit^{+} emerge which are CX3CR1-GFP^{-} (A1 subset) and CX3CR1-GFP^{+} (A2 subset). By E 10.5 both the A1 and A2 subsets have migrated to the head region and lowered c-kit expression (the only cells which express CX3CR1 in the CNS are the microglia). Furthermore, *in vitro* analysis showed that only the $CD45^{-}$c-kit^{+} subset was able to give rise to $CD45^{+}$ macrophages and erythrocytes - Erythro Myeloid Progenitors (EMPs). These $CD45^{-}$c-kit^{+} EMPs are thought to be the earliest precursors of microglia in the yolk sac. This comprehensive work also revealed two interesting details. Firstly, microglial development depends on the transcription factors Pu.1 and Irf8. Secondly, and counterintuitively, localization of microglia is unaffected (albeit delayed) in chemokine knockout mouse lines but is completely abrogated when Matrix metalloproteinase (MMP)-8 and MMP-9 are chemically inhibited (Kierdorf *et al.*, 2013).

The entry of microglia into the brain ends after the formation of the blood-brain barrier around E 12.0 (Risau and Wolburg, 1990). Microglia maintain their populations throughout adulthood through local proliferation and there is no significant contribution of circulating bone marrow-derived monocytes in the microglial population. It is interesting to note at this point that the depletion of microglia using radiation damages the blood-brain barrier and results in the infiltration of peripheral monocytes. In the absence of radiation, microglia renew exclusively from local pools after depletion (Bruttger *et al.*, 2015). Curiously, however, infiltrating myeloid precursor-derived macrophages which repopulate the brain post irradiation-induced depletion, retain a different transcriptional signature as well as an altered chromatin landscape. Functionally, they also differ in their response to inflammatory insults (Shemer *et al.*, 2018). This result was in stark contrast to data on alveolar macrophages (another embryonic resident macrophage population in the lungs) where repopulation of the

empty niche by adult circulating bone marrow-derived monocytes results in an almost complete acquisition of the alveolar macrophage fate (van de Laar *et al.*, 2016). This observation points to a possibility where the microglial state is the cumulative result of progressing through the rapidly changing neuroectoderm during development from early neurogenesis to gliogenesis and not just the final adult tissue (Hong *et al.*, 2016b).

1.3.1 Developmental and Pathogenic Roles of Microglia

Homeostatic resident adult microglia exhibit a ramified arboreal morphology with numerous dynamic extensions which they use for scanning the brain parenchyma. Consequently, one of their most visible functions was the phagocytosis of dying neurons-especially during development after sensing their presence through membrane contacts. Under homeostatic conditions have very limited mobility, moving only about 0.1 to 1.5μm per minute (Möller *et al.*, 2022). In addition to their “clean up” duties during development and in response to brain damage, microglia have also been shown to have an essential role in postnatal pruning and maturation of synapses directly implicating microglia in modifying the organisation of neural circuits (Paolicelli *et al.*, 2011; Schafer *et al.*, 2012).

The microglial state also shows strict temporal control with newly arrived microglia appearing highly proliferative and retaining their yolk sac signature. Over time, around postnatal day (P) 1 and P2 in mice, these microglia express genes associated with neurogenesis and neuronal migration possibly associated with their role in synaptic pruning and maturation. Later on during development and in the adult they adopt a state characteristic of homeostasis and immune surveillance described by the classic microglial markers Sall1, MafB, Selplg, and P2ry13 (Matcovitch-Natan *et al.*, 2016). Microglial pruning of synapses is also modulated by a fascinating mechanism involving the CD47 (a “don’t eat me” signal) and signal-regulatory protein alpha (SIRPα) where high neuronal expression of SIRPα at synapses blocks microglial SIRPα neuronal CD47 interaction allowing phagocytosis of synapses by microglia. Variations in the levels of neuronal SIRPα provides another layer of temporal control over the pruning of synapses by the microglia (Lehrman *et al.*, 2018; Jiang *et al.*, 2022). Further driving home the point, a subset of microglia receptive to GABA (γ-Aminobutyric acid) selectively prune

inhibitory synapses and modulate excitatory-inhibitory synapse ratio resulting in observable behavioural defects (hyperactivity) in the adult if this developmental function is compromised (Favuzzi *et al.*, 2021).

Microglia have also been shown to be exquisitely sensitive to the developmental state of the brain as well to their region of localization. In zebrafish, microglial entry into the developing brain happens preferentially through differentiating neurogenic areas and the microglia avoid areas with rapidly proliferating cells (Ranawat and Masai, 2021). Furthermore, in the same model, microglial are thought to be drawn-in in an IL34 and apoptotic-neuron-dependent manner (Ranawat and Masai, 2021). Microglia also show significant transcriptional heterogeneity based on the brain region of their residence with microglia in the cerebellum and hippocampus maintaining a more immune-alert state which is also accompanied by the necessary genes to support this heightened metabolic state (Grabert *et al.*, 2016).

Moving away from the homeostatic situation, neuroinflammatory conditions show the emergence of new microglial subsets and the downregulation of the core homeostatic microglial genes (described before) and upregulation of *Ccl2*, *Cxcl10*, *Ly86*, and *Mki67* indicative of active proliferation and chemokine production. Curiously, however, MHC II on microglia was not involved in antigen presentation to T cells during neuroinflammation (Jordão *et al.*, 2019).

Their loyalty to the CNS only goes so far as microglia often show pathogenic roles during neurodegenerative diseases (some reports do, however, also show roles for microglia in repair during demyelinating diseases like Multiple Sclerosis (Berghoff *et al.*, 2021). Case in point, microglia are known to be responsible for teaming up with complement proteins to effect early loss of synapses exhibited in mouse models of Alzheimer's disease (Hong *et al.*, 2016a). Adding to their pathogenic role, microglia have also been implicated in spreading amyloid-□ from regions of its accumulation to unaffected regions of the brain (Venegas *et al.*, 2017; d'Errico *et al.*, 2022).

The Microglial function then seems to range all the way from ensuring appropriate neuronal development and maturation of connections between neurons and housekeeping in cases of damage and cell death at one end to actively contributing to

neuropathology. This discrepancy is further amplified by the understanding that there is no “one” microglial state and that multiple subtypes of microglia can express the entire range of these functions meaning that all these processes are carried out by different cells at the same time. One thing is clear though, Microglia are highly dynamic and highly heterogeneous. This feature means that to understand a particular subset of microglia, it is necessary to isolate them in sufficient numbers at the exact right moment while minimising isolation-induced artefacts (Smith *et al.*, 2013). In line with this work, to study the developmental roles of microglia obtaining a large sample in the correct developmental window is difficult in mice and impossible for humans. I will use this opportunity to lead into the next section regarding the differentiation of iPSCs into microglia. These so-called iMicros (iMg) represent a unique opportunity to capture the developmental stages of and heterogeneity in microglia in an approach which is amenable to genetic as well as inhibitor-based perturbations.

1.3.2 iPSC-derived Microglia - iMicros

The first reports regarding the development of a protocol to generate human iPSC/ESC-derived microglia came from the laboratory of Dr. Rudolf Jaenisch at the Whitehead Institute. They utilized the embryoid body approach grown under low concentration of CSF-1 and IL34 (both ligands of CSF1R which is seen on the primitive yolk sac progenitors and also necessary for microglial proliferation and maturation). This allowed them to observe the formation of embryoid bodies displaying the presence of large cyst-like structures. When these cystic-EBs were plated, they grew out into lawns resembling endothelial cells which were in retrospect the haemogenic endothelia with their borders being positive for VE-cadherin, c-kit, CD41, and CD235a which are bonafide markers of primitive haemogenic endothelia (Hoeffel and Ginhoux, 2015). These endothelia when cultured over long durations (~1 month) in the presence of a low concentration of CSF-1 and a high concentration of IL34 resulted in the appearance of floating iMg cells (induced microglia). These floating iMg cells expressed the classical adult microglial markers TMEM119 and P2RY12. They were also highly phagocytic, proliferative, opsonized floating cotton fibre debris, and secreted a variety of chemokines when stimulated with LPS. Furthermore, they also acquired a transcriptional state closer to acutely isolated human microglia when cultured with

ESC-derived neurons as well as acquired a ramified morphology (Muffat *et al.*, 2016). Although this approach did generate large numbers of microglia, it required an extended differentiation duration of over 2.5 months. Furthermore, it relied on the stochastic generation of primitive haematopoietic progenitors consequently requiring multiple purification steps.

Haematopoiesis in mice and humans takes place in several transient waves until the ultimate establishment of HSCs in the bone marrow. They can (in mice) be briefly divided into Primitive haematopoiesis which happens in the extra-embryonic yolk sac and definitive haematopoiesis which happens in the haemogenic endothelia of the embryo proper. The latter generate Haematopoietic Stem Cells around E 9.5 (both mature and immature ones) which seed the fetal liver around E 10.5 following which the fetal liver becomes the dominant haematopoietic organ until late gestation (Hoeffel and Ginhoux, 2015). Based on this discussion, it is clear that both primitive and definitive haematopoiesis go through haemogenic endothelia but their respective progenitor pools as well as differentiation capacity differs greatly. However, the signals required for differentiation of ES cells along either primitive or definitive trajectories *in vitro* were not known. It was later uncovered in 2014 that the Wnt and Activin-Nodal signalling pathways played a crucial role in the determination of this developmental trajectory. This work started with the identification that CD235a was a marker for primitive haematopoietic progenitors henceforth described as receptor tyrosine kinase $KDR^{+}CD235a^{+}$. It further went on to identify that inhibition of wnt signalling during early mesodermal differentiation resulted in a large increase in the $CD235a^{+}$ population. Basically, inhibition of wnt signalling soon after patterning to the primitive streak mesoderm led to the generation of Primitive haematopoietic progenitors from human ES cells (Sturgeon *et al.*, 2014).

This identification of a patterning cue to direct human ESCs towards primitive haematopoiesis led to more accurate directed differentiation protocols which did not rely on the spontaneous generation of haemogenic endothelia in embryoid bodies. Consequently, they resulted in significantly higher efficiencies of differentiation, lesser purification steps, as well as shorter differentiation durations. I will now discuss two of the most recent protocols to generate iMg cells from human ES cells (look out for activation and inhibition of wnt signalling).

Abud et al. differentiated human iPSCs to microglia initially by patterning to the primitive streak mesoderm and primitive haematopoietic progenitors under hypoxic conditions (5% O_2, 5% CO_2, and 90% N_2) by treatment with BMP4 (a known mesodermal patterning agent) and Activin-A (activates activin-nodal signalling, see above). Once pattered, they expand the haemogenic endothelia using media supplemented with VEGF, FGF2, IL3, IL6, SCF (Stem Cell Factor), and TPO (human Thrombopoietin) taking 10 days to differentiate human iPSCs into haematopoietic progenitor cells. After sorting for haematopoietic progenitor cells, they initiated microglial differentiation in the presence of CSF-1, IL34, and TGF□. Finally, to simulate the CNS environment, they further matured the microglia in the presence of CD200 and CXCL1 (ligands commonly expressed on neurons in the CNS) taking a total of 38 days starting from iPSCs. The generated iMg cells were similar to fetal as well as adult microglia, expressed microglia-specific markers like PU.1, TREM2, P2RY12, and $CD11b^{int}/CD45^{lo-int}$, and mounted a cytokine response to LPS stimulation (Abud *et al.*, 2017).

Guttikonda et al. utilized modulations to the Wnt signalling to differentiate iPSCs into microglia. They observed that transient activation of Wnt signalling using the □-secretase inhibitor CHIR99021 for 18-24 hours followed by continuous Wnt inhibition using the porcupine inhibitor IWP2 coupled with Nodal signalling activation using Activin-A, and BMP4 managed to generate a large number of $KDR^{+}CD235a^{+}$ primitive haematopoietic progenitors in the absence of extended periods of hypoxia. Even without sorting, they observed a large number of floating cells above the haemogenic endothelium - after growing the haematopoietic progenitors for a week in media supplemented with the haematopoietic cytokines mentioned above - of which 60% had a bonafide haematopoietic identity. They then matured the iMg cells by 10 days of co-culture with cortical neurons. By the end of the co-culture duration, all the cells were positive for the microglial marker CD11B and PU.1 with a large majority also being positive for CX3CR1 (Guttikonda *et al.*, 2021).

It is clear then that both these methods effectively produce microglia-like cells from iPSCs at very high efficiency. The choice of protocol then depends on the access to hypoxia as well as the preferred means of maturation and the experimental timescales used. For our microglia, the protocol used is a novel approach developed in the lab and

described in Takata et al. and described in the Results and Methods sections. The microglia that we generate are then introduced into our brain organoids to measure their effects on neurodevelopment as well as their effects on the proliferation and maturation of the different cell types generated in the brain organoid. This adds to previous observations that organoids co-cultured microglia are the most similar to their *in vivo* counterparts and cause downregulation of interferon and stress-related genes in human radial glial cells in the organoid (Popova *et al.*, 2021).

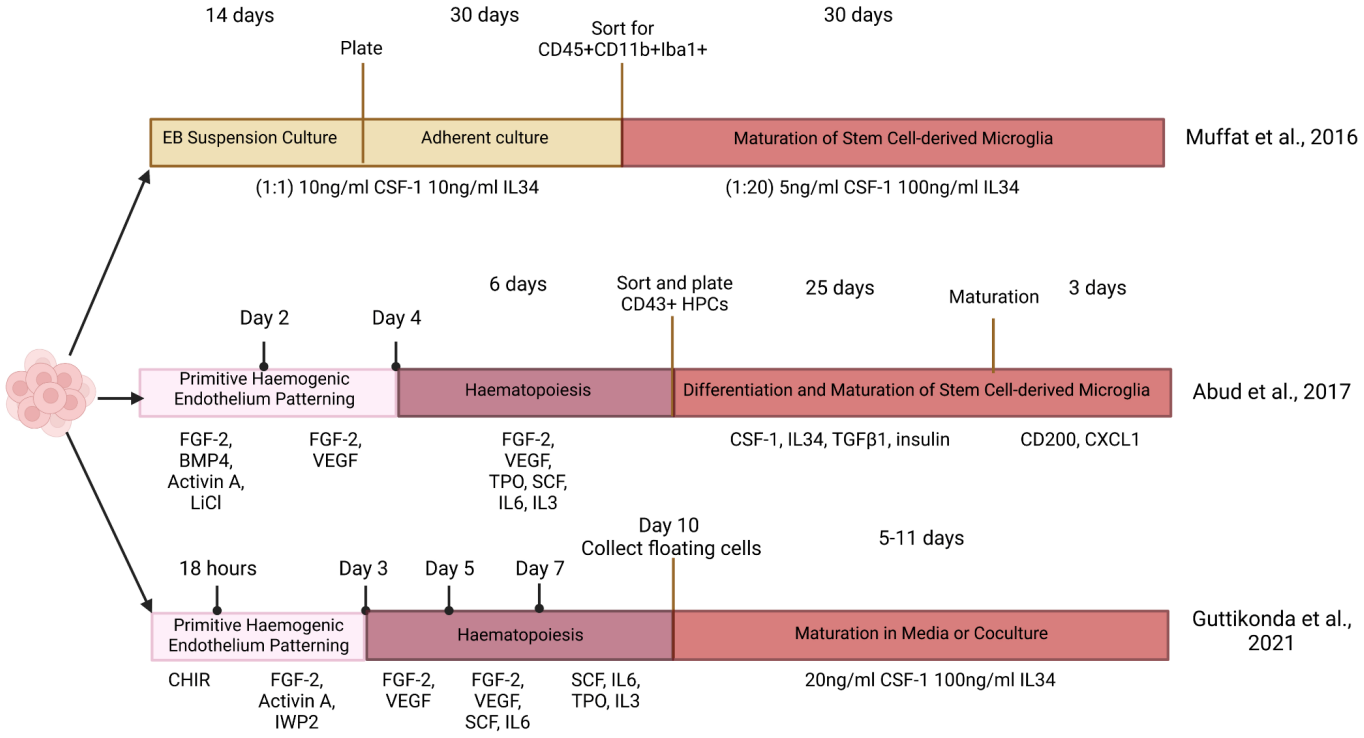

Fig. 1.4: Comparisons of the protocols used to generate iPSC/ ESC-derived microglia: Please note the differences in the lengths of the protocols as well as the need for sorting. TPO: Human Thrombopoietin, CHIR: CHIR99021 Wnt agonist, IWP2: Wnt inhibitor, SCF: Stem Cell Factor, VEGF: Vascular Endothelial Growth Factor, FGF-2: Fibroblast Growth Factor-2, CSF-1: Macrophage Colony Stimulating Factor-1, BMP4: Bone Morphogenetic Protein-4, and TGFβ1: Transforming Growth Factor beta 1.

Although these iPSC-derived microglia supply an immune compartment to the brain organoids and the microglial role in affecting neurodevelopment is very interesting and warrants further study, integration of endothelial cells and pericytes in the form of vessels in brain organoids provides an interesting avenue for increasing the complexity

of brain organoids. Furthermore, the possibility of developing functioning perfusion in the long term provides further encouragement for the development of vascularized brain organoid models. Before I move on to a description of the project, I will provide a very short description of blood vessels and then move on to the idea of the project.

1.4 iPSC-derived Blood Vessels and the idea behind this Project

The integration of blood vessels into organoids and the establishment of a functional circulatory system have been the goals of developmental biologists and tissue engineers for a long time. The latter goal will require long-term collaborations between biologists, biotechnologists and tissue engineers and hence will not be discussed further in this thesis. The former is the problem we have decided to tackle in this work.

Vascularization of Organoids can take two main directions. Firstly, vascularization by *in vivo* transplantation - where the hiPSC-derived organoid is grafted into a mouse and the mouse blood vessels invade the organoid (requiring angiogenesis), and secondly *in vitro* vascularization which involves neovasculogenesis as well as angiogenesis. A beautiful example of the former is the work by *Mansour et al.* where brain organoids cultured *in vitro* for around 50 days were grafter into the before intracerebral implantation in NOD-SCID (non-obese diabetic severe combined immunodeficiency) mice. The grafter organoids survived for over 7 months post-transplantation, displayed progressive differentiation with appropriately organized progenitor zones, and vascularization by mouse $CD31^{+}$ (an endothelial cell marker) blood vessels. These organoids also showed microglial invasion by mouse-derived cells and displayed greater differentiation and maturation of neurons as compared to stage-matched *in vitro* cultured organoids. Furthermore, after extensive vascularization almost no apoptotic signals were observed in the *in vivo* organoids compared to large amounts of apoptosis in culture (Mansour *et al.*, 2018).

Although *in vivo* transplantation is an excellent way for organoid vascularization, the requirement of specialised surgical skills as well as the inability to integrate cytokine signals as well as cells of human origin results in undefined conditions and confounding results. As a result, there has been much recent focus on *in vitro* vascularization

approaches using either primarily isolated or hiPSC-derived blood vessel-forming cells. However, difficulties in obtaining genotype-matched iPSCs and primary cells cause complications in the study of microglial (immune) involvement in the developmental processes (Takebe *et al.*, 2014). This is why, in this project, we decided to use iPSC-derived blood vessels to vascularize our brain organoids.

The idea and methodology for generating vascularized brain organoids were first described in a very recent paper by Sun et al. who used human ES cell-derived blood vessel organoids and fused them together with brain organoids giving rise to vascularized brain organoids in addition to functional microglial cells (Sun *et al.*, 2022). However, we faced certain complications (discussed in later sections) during our implementation of their protocol and had to develop our own novel protocol for iPSC-derived vascularized organoids. Blood vessels do not consist only of endothelial cells but require the tandem formation of endothelial cells as well as pericytes. This tandem formation differed from the goal of most plate-based protocols which generate high percentages of pure endothelial cells (Patsch *et al.*, 2015). As a concomitant generation of endothelial cells and pericytes was necessary in our model, we identified in the literature a protocol by Wimmer et al. which generated human blood vessel networks from iPS/ES cells and optimized their fusion with our brain organoids (Wimmer *et al.*, 2019b, 2019a; Nikolova *et al.*, 2022). We observed the formation of bonafide vessel-like structures and integrated iPSC-derived microglia into these fusion organoids at a biologically relevant time point. We then used a combination of sectioning, confocal microscopy, and flow cytometry to establish the successful formation of this vascularized brain organoid model.

This project is designed to be an exploratory study of the role microglia might play in the vascularization of the brain during development. Based on previous evidence in the literature, macrophages and microglia have been shown to increase blood vessel sprouting and extension, especially under hypoxic/ischemic conditions, we hypothesised that the hypoxic core of our organoids would influence the co-cultured microglia to draw and increase the sprouting in the integrated blood vessels (Rymo *et al.*, 2011; Anandi *et al.*, 2023). Our model would also enable further research in the identification of novel vessel associations of microglia or the effects of endothelial cell-derived factors on microglial and neuronal differentiation. In the broader scheme of

things, adaptations of our models to angiogenesis in tumour cell-derived organoids as well as investigations of vascularization defects in models of neurodevelopmental disorders provides an avenue for *in vitro* study of this narrow developmental window under completely defined culture conditions.

2. Materials and Methods

2.1 Materials and Reagents:

Reagent or Resource	Source	Identifier
Media		
DMEM/F12	ThermoFischer Scientific	Cat # 11320033
Neurobasal	ThermoFischer Scientific	Cat # 21103049
mTeSR Plus	Stemcell Technologies	Cat # 1000276
StemPro-34 SFM	ThermoFischer Scientific	Cat # 10639011
IMDM	ThermoFischer Scientific	Cat # 31980030
STEMdiff APEL 2	Stemcell Technologies	Cat # 05270
Endothelial Cell Growth Medium MV2	PromoCell	Cat # C-39226
Nutrient Supplements		
MEM-NEAA	ThermoFischer Scientific	Cat # 11140050
Glutamax	ThermoFischer Scientific	Cat # 35050061
L-glutamine	ThermoFischer Scientific	Cat # 25050081
N2 Supplement	ThermoFischer Scientific	Cat # 17502048
B27 Supplement	ThermoFischer Scientific	Cat # 17504044
B27-Vit A Supplement	ThermoFischer Scientific	Cat # 17502048
Knockout™ Serum Replacement	ThermoFischer Scientific	Cat # 10828028
Chemicals, Peptides, and Recombinant Proteins		
Recombinant Human Insulin	Sigma-Aldrich	Cat # 19278-5ML
Recombinant Human BMP4	RnD	Cat # 314-BP
Recombinant Human FGF-2	RnD	Cat # 233-FB

Recombinant Human VEGF	RnD	Cat # 293-VE
Recombinant Human IL6	RnD	Cat # 206-IL
Recombinant Human IL3	RnD	Cat # 203-IL
Recombinant Human DKK1	RnD	Cat # 5439-DK
Recombinant Human SCF	RnD	Cat # 255-SC
Recombinant Human CSF-1	RnD	Cat # 216-MC
Recombinant Human Transferrin	Roche	Cat # 10652202001
Ascorbic Acid	Sigma-Aldrich	Cat # A4544
1-Thioglycerol (MTG)	Sigma-Aldrich	Cat # M6145
Penicillin-Streptomycin	ThermoFischer Scientific	Cat # 15140122
Antibiotic-Antimycotic	ThermoFischer Scientific	Cat # 15140122
2-Mercaptoethanol	ThermoFischer Scientific	Cat # 2337545
Dorsomorphin	TOCRIS	Cat # 3093
A83-01	TOCRIS	Cat # 2939
SB431542	TOCRIS	Cat # 1614
LDN-193189	TOCRIS	Cat # 6053
Forskolin	Selleck Chemicals	Cat # S2449
CHIR99021	TOCRIS	Cat # 4423
Y27632 ROCK inhibitor	Merck Millipore	Cat # SCM075
Matrigel	Corning	Cat # 354277, 354234, 356237

Antibodies

Reagent or Resource	Source	Identifier
Goat anti-SOX2	RnD	Cat # AF2018
Rabbit anti-SOX2	Abcam	Cat # AB97959
Chicken anti-MAP2	Abcam	Cat # AB92434

Rabbit anti-CD31	Abcam	Cat # AB28364
Mouse Anti-VGLUT2	Abcam	Cat # AB211869
Rabbit Anti-PSD95	Abcam	Cat # 18258
Mouse anti-CD45	BioLegend	Cat # 368516
Mouse anti-CD14	BioLegend	Cat # 325604, 301834
Mouse anti-CD11b	BD Biosciences	Cat # 557918
Mouse anti-CD163	BD Biosciences	Cat # 562670
Mouse anti-CXCR4	BioLegend	Cat # 306516
Mouse anti-CD44	BioLegend	Cat # 338806
Mouse anti-CD271	BD Biosciences	Cat # 743358
Mouse anti-CD24	BD Biosciences	Cat # 561646
Mouse anti-CD15	BioLegend	Cat # 323034
Rat anti-CX3CR1	BioLegend	Cat # 341626, 341608
Mouse anti-CD31	BD Biosciences	Cat # 560983
Mouse anti-CD31	BioLegend	Cat # 303115
Mouse anti-CD144b	BD Biosciences	Cat # 561714

2.2 Media composition

mTeSR™ Plus

The mTeSR™ Plus complete medium was prepared by mixing 100ml of mTeSR™ Plus 5x Supplement (stored at -20°C) into 400ml of mTeSR™ Plus Basal Medium (stored at 4°C) according to manufacturers instructions and split into 40ml aliquots.

2-mercaptoethanol dilution (1:100), 100µl

A working solution of 2-mercaptoethanol was prepared by aseptically adding 1µl of 2-mercaptoethanol to 99µl of DMEM/F-12 and using it immediately after preparation.

Human Embryonic Stem Cell (hESC) Media (Prepared according to (Lancaster and Knoblich, 2014))

For 50ml of hESC medium, 40ml of DMEM/F-12, 10ml KnockOut™ Serum Replacement, 1.5ml Fetal Bovine Serum (FBS), 500µl Gibco™ MEM Non-Essential Amino Acids Solution (100x), 500µl Gibco™ GlutaMAX™ Supplement (100x), and 35µl 2-mercaptoethanol dilution were combined together. This was followed by filtering the medium through a Merck Millex® 33mm syringe filter. The media was stored at 4ºC for up to 2 weeks.

Serum-Free Human Embryonic Stem Cell (SF-hESC) Media (Prepared according to (Wimmer *et al.*, 2019b))

For 50ml of SF-hESC medium, 40ml of DMEM/F-12, 10ml KnockOut™ Serum Replacement, 500µl Gibco™ MEM Non-Essential Amino Acids Solution (100x), 500µl Gibco™ GlutaMAX™ Supplement (100x), and 35µl 2-mercaptoethanol dilution were combined together. This was followed by filtering the medium through a Merck Millex® 33mm syringe filter. The media was stored at 4ºC for up to 2 weeks.

Neural Induction Media (NIM) (Prepared according to Lancaster and Knoblich, 2014)

For 40ml of NIM, 38ml of DMEM/F-12, 400µl Gibco™ GlutaMAX™ Supplement (100x), 400µl Gibco™ MEM Non-Essential Amino Acids Solution (100x) were combined together, and Heparin was added to a final concentration of 1µg ml^{-1}. This was followed by filtering the medium through a Merck Millex® 33mm syringe filter. Post filtration, 400µl of Gibco™ N2 Supplement (100x) was added. The media can be stored at 4ºC for up to 2 weeks.

Organoid Differentiation Medium without Vitamin A (ODM-VitA) (Prepared according to Lancaster and Knoblich, 2014)

For 40ml of ODM-VitA, 19ml DMEM/F-12,19ml Neurobasal Medium, 400µl Gibco™ GlutaMAX™ Supplement (100x), 400µl Gibco™ Penicillin-Streptomycin (10,000U ml^{-1}) (100x), 200µl Gibco™ MEM Non-Essential Amino Acids Solution (100x), 10µl Human Insulin Recombinant Protein Solution (Sigma-Aldrich), and 14µl 2-mercaptoethanol dilution were combined together. This was followed by filtering the medium through a

Merck Millex® 33mm syringe filter. Post filtration, 400µl of Gibco™ N2 Supplement (100x) and 800µl Gibco™ B-27™ Supplement (50X), minus vitamin A were added. The media was stored at 4ºC for up to 2 weeks.

Organoid Differentiation Medium with Vitamin A (ODM+VitA) (Prepared according to Lancaster et al ((Lancaster and Knoblich, 2014))

For 40ml of ODM-VitA, 19ml DMEM/F-12,19ml Neurobasal Medium, 400µl Gibco™ GlutaMAX™ Supplement (100x), 400µl Gibco™ Penicillin-Streptomycin (10,000U ml^{-1}) (100x), 200µl Gibco™ MEM Non-Essential Amino Acids Solution (100x), 10µl Human Insulin Recombinant Protein Solution (Sigma-Aldrich), and 14µl 2-mercaptoethanol dilution were combined together. This was followed by filtration through a Merck Millex® 33mm syringe filter. Post filtration, 400µl of Gibco™ N2 Supplement (100x) and 800µl Gibco™ B-27™ Supplement (50X), serum-free were added. The media can be stored at 4ºC for up to 2 weeks.

N2B27 Medium (Prepared according to Wimmer et al, 2019b)

For 40ml of N2B27 Medium, 20ml DMEM/F-12, 20ml Neurobasal Medium, 200µl Gibco™ GlutaMAX™ Supplement (100x), and 28µl of 2-mercaptoethanol dilution were combined together. This was followed by filtration through a Merck Millex® 33mm syringe filter. Post filtration, 200µl of Gibco™ N2 Supplement (100x) and 400µl Gibco™ B-27™ Supplement (50X), minus vitamin A were added. Media can be stored at 4ºC for up to 2 weeks.

SP+ Medium

For 40ml SP+ medium, combine together 39.6ml complete StemPro™-34 SFM and 400µl Gibco™ Penicillin-Streptomycin (10,000U ml^{-1}) (100x). Keep in the dark and store at 4ºC.

SP++ Medium

For 40ml SP++ medium, SP+ medium was supplemented with Human Recombinant Transferrin, Ascorbic acid, L-glutamine, and 1-Thioglycerol. The media was kept in the dark and stored at 4ºC.

SF-Diff Medium

For 40ml SF-Diff medium, 30ml IMDM, 10ml DMEM/F-12, 400µl Gibco™ Penicillin-Streptomycin (10,000U ml^{-1}) (100x) were combined together and BSA (Bovine Serum Albumin) was added to a final concentration of 0.05%. The medium was then filtered through a Merck Millex® 33mm syringe filter. Post filtration, 400µl of Gibco™ N2 Supplement (100x) and 800µl Gibco™ B-27™ Supplement (50X), serum-free were added.

FACS Buffer

The FACS Buffer is prepared by supplementing 1l PBS with BSA to a final concentration of 0.5% and EDTA to a final concentration of 2mM.

2.3 Methods

2.3.1 Human iPSC culture and maintenance

hiPSCs were cultured on Costar® 6-well Clear TC-treated Multiple Well Plates which were coated with Corning® Matrigel® Growth Factor Reduced (GFR) Basement Membrane Matrix (Matrigel). Briefly, each well of the 6-well plate was coated with a cold 1% solution of matrigel in PBS while using chilled 1000µl pipette tips. Transfer the plates into a 37ºC incubator for polymerization of the matrigel matrix for 1-24hrs.

hiPSCs were maintained on matrigel-coated plates at 37ºC in a Forma™ Steri-Cycle™ CO2 184L Humidified Incubator at 5% CO_2 - air in 2ml/well mTeSR™ Plus medium. Media was changed daily by tilting the plate and minimising contact between the tip of the serological pipette and matrigel coating. Culture quality was ensured by regular assessment of colony morphology with smooth edges, densely packed cells, and large prominent nucleoli within individual cells.

Cells were passaged every 5-6 days using ReLeSR™. Briefly, 70-80% confluent wells of hiPSCs (colonies just about to touch) were washed with 2ml/well of Cytiva HyClone™ Dulbecco's Phosphate Buffered Saline (DPBS) solution. 1ml of ReLeSR™ was added

per well and incubated at RT for not more than 1 min. The ReLeSR™ solution was aspirated and the plates were transferred to 37°C for 1.5min with the choice of time point made by observations of colony boundary recession and brightening as well as the appearance of gaps in tightly packed colonies. 1ml mTeSR™ was added along the side of the well and the plates were tapped gently for about 30sec. The iPSCs detach as colonies which are then transferred to a 15ml falcon tube and triturated at most 2-3 times using a 1000µl pipette tip. They are then seeded into new matrigel coated, mTeSR™ containing 6 well plates at 1:50 to 1:100 split ratios.

2.3.2 Induced (iPSC-derived) Primitive Macrophage (iMac) Differentiation

The iMacs were generated according to the protocol described in *Takata et al., 2017*. Briefly, the cells were seeded onto matrigel-coated plates and allowed to adhere completely in a conventional 5% CO_2 air tissue culture incubator. The next day the cells were patterned towards the primitive streak mesoderm by culturing in SP++ medium supplemented with 5ng/ml BMP4, 2µM CHIR99021, and 50ng/ml VEGF. On Day 2, the medium was changed to SP++ supplemented with 5ng/ml BMP4, 20ng/ml FGF-2, and 50ng/ml VEGF. On Day 4, the medium was changed to SP++ supplemented with 15ng/ml VEGF and 20ng/ml FGF-2. Days 2 to 6 showed a rapid proliferation in the cell layer and showed complete coverage of the plate surface by the Haemogenic endothelium on Day 6. Between Days 6 - 12, the cells were cultured in SP++ medium supplemented with 20ng/ml VEGF, 20ng/ml FGF-2, 20ng/ml IL6, 40ng/ml IL3, 60ng/ml Wnt antagonist DKK1 (Dickhopf WNT signalling pathway inhibitor 1), and 100ng/ml SCF. The addition of DKK1 serves to drive primitive haematopoiesis. Between Days 12 - 16, the cells were cultured in SP++ supplemented with 20ng/ml FGF-2, 20ng/ml IL6, 40ng/ml IL3, and 100ng/ml SCF to drive primitive myelopoiesis. DKK1 is discontinued at this stage after robust induction of primitive haematopoiesis. Floating cells begin to appear in the culture usually after the first 6 days. These cells are collected by centrifugation at RT for 5 min at 1200rpm and added back to the wells with fresh media. From Day 16 onwards until Day 26, the media was switched to SF-Diff supplemented with 50ng/ml CSF-1 to promote the maturation of primitive macrophages from the floating myeloid progenitors. From Day 19 onwards floating clumps - a telltale sign of myeloid identity - of iMacs begin to appear. The cells were cultured under hypoxia for

the first 8 days (Day 0 - 8) and then returned to a conventional 5% CO_2 air tissue culture incubator. The identity of these cells was established using flow cytometry on Day 26.

2.3.3 Brain organoid differentiation: Lancaster and DS

Brain Organoid protocol modified from Lancaster and Knoblich, 2014.

Start with one well of 70-80% confluent iPSCs exhibiting less than 5% differentiation detected by observations of colony morphology. On Day 0, the old mTeSR™ Plus medium was aspirated and the well was washed with 2ml PBS and the PBS was aspirated. In parallel, 500µl of StemPro™ Accutase™ was warmed to 37ºC in a water bath and added to the well. The plate was then incubated in a normoxia incubator at 37ºC for 5min. **Incubation for more than 6 minutes is not recommended as it can lead to excessive cell death.** The Accutase™ was quenched by the addition of 500µl mTeSR™ Plus medium. The cells were collected in a 15ml tube and spun down at 1200rpm for 5min at 20ºC and the supernatant was discarded. The pellet was resuspended in 1ml hESC medium by triturating using a 1000µl pipette at most 4-5 times to get a single-cell suspension. **Trituration more than 6 times or with more force is highly discouraged as this will cause excessive cell death and poor aggregation.** The cells were counted using Invitrogen™ Countess™ Automated cell counter.

The organoids were seeded in a Corning® 96-well Clear Round Bottom Ultra-Low Attachment Microplate to ensure forced aggregation of the iPSCs with ~150µl media per well. Brain Organoid aggregation media was prepared by supplementing hESC media with a low FGF-2 concentration (5ng/ml) and 20µM ROCK inhibitor (this prevents apoptosis in iPSC single cell suspension). The counted cell suspension was added to the aggregation media to ensure the seeding of ~9,000 iPSCs per well and mixed gently using a 10ml serological pipette. 150µl of this mixture was individually added to each well of the 96-well plate and the plates were left undisturbed for 2 days at 37ºC and normoxia. On Day 2, 150µl of aggregation medium (identical in composition to Day 0) was topped up in each well taking care not to disrupt the embryoid body formed at the bottom of the well. On Day 4, the organoids were observed carefully to look for signs of brightening (see Results section) and half the media was gently aspirated taking care

not the suck in the organoid at the bottom and was replaced with aggregation media without ROCK inhibitor. The embryoid bodies were observed closely between Days 4-6 to ensure signs of brightening as well as a size between 500-600µm. On Day 6, the embryoid bodies were transferred using a cut 200µl pipette tip with a 1-1.5mm tip diameter to either a 96-well round bottom ultra-low attachment plate with 275ul Neural Induction Media (NIM) or to a Costar® 24-well Clear Flat Bottom Ultra-Low Attachment Plate with 500µl NIM. This NIM was half-replaced every 2 days until Day 11-12 as judged by the observation of a radially organized bright region along the periphery of the aggregate indicative of neuroectodermal differentiation. The aggregates at this stage should display smooth bright boundaries with no signs of fragmentation. Only pick the most pristine aggregates for the next embedding step.

Brain Organoids by Dual SMAD inhibition as modified from (Sun *et al.*, 2022)

This protocol was exactly identical to the protocol described above. The difference was in the seeding of ~7,000 cells/well as opposed to ~9,000 along with a ROCK inhibitor concentration of 10µM on Day 0. The next, and more major difference, was in the media compositions. On Day 2, the entirety of the old media was aspirated and hESC media was supplemented with 2.5µM Dorsomorphin and 2µM A83-01 followed by a half replacement on Day 4. On Day 6, the embryoid bodies were carefully observed for signs of brightening before transferring with cut 200µl tips to NIM supplemented with 10µM SB431542 and 200nM LDN193189. During Neural induction, check for the same signs as above and the media was half replaced every 2 days until Day 11-12.

Matrigel Embedding and Organoid Differentiation modified from (Lancaster and Knoblich, 2014)

The Day 11-12 aggregates were transferred onto a STEMCELL™ Organoid Embedding Sheet with a cut 200µl tip having a hole diameter of 1.5-2.0mm. The residual media was aspirated taking care to point the pipette tip away from the organoid to prevent sucking in the organoid into the tip. Small aliquots ~200µl of Growth-factor reduced Matrigel were maintained on ice and using a chilled 200µl pipette tip, a 14µl droplet of cold matrigel was added. It was important at this stage to work in batches to ensure the aggregates do not dry out as well as to prevent premature polymerization of the

matrigel. The matrigel encased aggregates were allowed to polymerize for 25-30min at 37ºC. The matrigel droplets containing the aggregates were then dislodged using slight media pressure with a 1000µl pipette and grown in a Corning® 100 mm TC-treated Culture Dishes containing 15ml ODM-VitA in normoxia at 37ºC with the media half replaced two days later. On Day 15-16 (4 days after matrigel embedding), the ODM-VitA was replaced with ODM+VitA and the plates were placed on an orbital shaker to ensure improved nutrient absorption set at 78rpm and the media was half-replaced every 2 days. On Day 20 of Organoid differentiation, shear off the matrigel droplet using a 1000µl pipette tip with an opening smaller than the diameter of the matrigel droplets. Grow the organoids until Day 26.

2.3.4 Blood Vessel Organoid Protocol Development - All Protocols

A large number of different protocols were applied to generate hiPSC-derived blood vessel organoids. Instead of writing in a paragraph, their differences are most clearly seen in table format as seen in Table 1 (Patsch *et al.*, 2015; Wimmer *et al.*, 2019b, 2019a; Abutaleb and Truskey, 2021; Hamad *et al.*, 2022; Nikolova *et al.*, 2022; Sun *et al.*, 2022). Based on the information obtained from the flow cytometry-based identification of CD31+ endothelial cell induction using these protocols, we developed an optimized protocol for the high-efficiency generation of Blood Vessel Organoids which is described in detail in the Table.

<table>
<tr><td>Day</td><td colspan="3">Protocol</td></tr>
<tr><td></td><td>1</td><td>2</td><td>3</td></tr>
<tr><td>0</td><td colspan="3">Seed 9000 cells per well, 150µl hESC medium, 10µM ROCK inhibitor</td></tr>
<tr><td>1</td><td colspan="3"></td></tr>
<tr><td>2</td><td rowspan="2">APEL2 + 6µM CHIR99021</td><td rowspan="2">APEL2 + 12µM CHIR99021 + 30ng/ml BMP4</td><td rowspan="2">APEL2 + 12µM CHIR99021 + 30ng/ml BMP4</td></tr>
<tr><td>3</td></tr>
<tr><td>4</td><td rowspan="3">APEL2 + 50ng/ml VEGF + 25ng/ml BMP4 + 10ng/ml FGF-2</td><td rowspan="3">APEL2 + 50ng/ml VEGF + 25ng/ml BMP4 + 10ng/ml FGF-2</td><td rowspan="3">APEL2 + 100ng/ml VEGF + 2µM Forskolin (dissolved in Ethanol)</td></tr>
<tr><td>5</td></tr>
<tr><td>6</td></tr>
<tr><td>7</td><td colspan="3" rowspan="5">MV2 + 50ng/ml VEGF</td></tr>
<tr><td>8</td></tr>
<tr><td>9</td></tr>
<tr><td>10</td></tr>
<tr><td>11</td></tr>
<tr><td>12</td><td colspan="3" rowspan="4">Embed in 14µl Matrigel droplet, ODM-VitA + 20ng/ml VEGF</td></tr>
<tr><td>13</td></tr>
<tr><td>14</td></tr>
<tr><td>15</td></tr>
</table>

<table>
<tr><td>Day</td><td colspan="4">Protocol</td></tr>
<tr><td></td><td colspan="4"></td></tr>
<tr><td></td><td>4</td><td>5</td><td>6</td><td>7</td></tr>
<tr><td>0</td><td colspan="3">Seed 7000 cells per well, 150µl SF-hESC medium, 50µM ROCK inhibitor</td><td>Seed 400 cells per well, 150µl SF-hESC medium, 50µM ROCK inhibitor</td></tr>
<tr><td>1</td><td></td><td></td><td></td><td></td></tr>
<tr><td>2</td><td rowspan="2">APEL2 + 6µM CHIR99021</td><td>APEL2 + 6µM CHIR99021</td><td rowspan="3">N2B27 + 12µM CHIR99021 + 30ng/ml BMP4</td><td rowspan="3">N2B27 + 12µM CHIR99021 + 30ng/ml BMP4</td></tr>
<tr><td>3</td><td>APEL2 (STOP CHIR99021)</td></tr>
<tr><td>4</td><td rowspan="3">APEL2 + 200ng/ml VEGF + 25ng/ml BMP4 + 100ng/ml FGF-2</td><td rowspan="3">APEL2 + 300ng/ml VEGF + 200ng/ml FGF-2</td></tr>
<tr><td>5</td><td rowspan="2">N2B27 + 300ng/ml VEGF + 200ng/ml FGF-2</td><td rowspan="2">N2B27 + 300ng/ml VEGF + 200ng/ml FGF-2</td></tr>
<tr><td>6</td></tr>
<tr><td>7</td><td colspan="2" rowspan="5">MV2 + 100ng/ml VEGF</td><td rowspan="4">Embed in 14µl Matrigel droplet, ODM-VitA + 100ng/ml VEGF + 100ng/ml FGF-2</td></tr>
<tr><td>8</td></tr>
<tr><td>9</td></tr>
<tr><td>10</td></tr>
<tr><td>11</td><td rowspan="6">Switch Medium to ODM+VitA + 100ng/ml VEGF + 100ng/ml FGF-2</td></tr>
<tr><td>12</td><td colspan="2" rowspan="4">Embed in 14µl Matrigel droplet, ODM-VitA + 20ng/ml VEGF</td></tr>
<tr><td>13</td></tr>
<tr><td>14</td></tr>
<tr><td>15</td></tr>
<tr><td>16</td><td colspan="3">Switch to ODM+VitA + 20ng/ml VEGF</td></tr>
</table>

Table 1: Comparison of the different endothelial cell/blood vessel organoid generation protocols in literature (excludes the currently used protocol, which is described in greater detail in the next section)

2.3.5 Protocol for the generation of Blood Vessel Organoids

The iPSC cell suspension was prepared in a manner identical to that mentioned in the protocol for brain organoids and spun down. This time, however, the pellet was resuspended in 1ml SF-hESC medium and triturated using a 1000µl pipette at most 2 times. The cell suspension was then counted using an Invitrogen™ Countess™ Automated cell counter.

The organoids will be seeded in a Corning® 96-well Clear Round Bottom Ultra-Low Attachment Microplate to ensure forced aggregation of the iPSCs with ~100µl SF-hESC media per well. The SF-hESC media was supplemented with 50µM ROCK inhibitor. A measured volume of cell suspension was added to it to ensure ~200 cells per well of the 96-well plate and mixed on the lowest pipette-aid setting at most 4 times. **This step was performed as gently as possible or the iPSCs might fail to form healthy aggregates in the wells**. While working fast, 100µl of this mixture was added to each well of the 96-well plate and left undisturbed for 24 hours. The aggregates should measure between 50-100µm and display smooth borders after 24 hours. If aggregates appeared small they were allowed another 24-36 hours of aggregation before proceeding with the next step.

Once the aggregates have met the prior stated quality requirements, mesoderm induction was initiated (Day 0). The media in the well was aspirated without disturbing the aggregate and replaced with ~250µl/well of N2B27 medium supplemented with 30ng/ml BMP4 and 12µM CHIR99021 taking care not to disrupt the aggregate. The plate was left undisturbed for 3 days. The aggregates were checked after mesoderm induction (Day 3) to ensure smooth boundaries and a bright appearance under the light microscope. The old media was aspirated and replaced with ~250µl/well of N2B27 medium supplemented with 100ng/ml VEGF and 2µM Forskolin (dissolved in DMSO at a 20mm concentration to minimise the amount of DMSO in the final medium) and left undisturbed for 2 more days. The aggregate was observed daily after this point and showed signs of surface darkening due to cell death caused by the forskolin but maintained its integrity. On Day 5, all the aggregates were pooled together in an Eppendorf™ microcentrifuge tube and allowed to settle to the bottom under gravity. The supernatant was then aspirated and the tube was chilled on ice. Finally, using chilled 200µl pipette tips, 14µl/droplet of ice-cold matrigel was added to the tube, the “aggregate slurry” was mixed 5-10 times using a cut 200µl chilled pipette tip, and a 14µl drop of matrigel containing the aggregates was deposited onto the cavities of the STEMCELL™ Organoid Embedding Sheet or fused with iPSC-derived Brain Organoids (next section). The steps after this and the media compositions were identical to those used in the protocol on brain organoids with additional supplementation of 100ng/ml VEGF and 100ng/ml FGF-2 at each stage. The embedded aggregates were then

observed daily to spot signs of vessel sprouting (see Results section) from the core of the organoid which usually appeared within 2-3 days.

2.3.6 Fusion of Brain and Blood Vessel Organoids

The above protocol for the generation of blood vessel organoids results in aggregates which are ~100-200μm in diameter - too small to orient manually with the naked eye. To overcome this obstacle, Day 12 brain organoids were deposited onto the STEMCELL™ Organoid Embedding Sheet and the residual media was aspirated. Working fast, the "aggregate slurry" was prepared to ensure 3-4 Day 5 blood vessel organoids per 14μl matrigel droplet and mixed with a chilled cut 200μl tip. The matrigel droplet was then deposited onto the brain organoids and allowed to polymerize as before. Following this, all steps were identical to the protocol for the generation of blood vessel organoids. These embedded aggregates were observed daily with particular attention to the absence of excessive sprouting from properly differentiated brain organoids.

2.3.7 Co-culture of Brain/ Fused vascularized brain organoids with iPSC-derived primitive macrophages

The iMacs were introduced into the Brain/ Vascularized brain organoids using a co-culture strategy where they will mature in the neuronal environment similar to CNS into iMicroglia. Day 26 organoids were transferred from Corning® 100 mm TC-treated Culture Dishes using cut 1000μl pipette tips into Costar® 24-well Clear Flat Bottom Ultra-Low Attachment Plate containing 1ml ODM+VitA supplemented with 50ng/ml M–CSF (in the case of brain organoids) or 50ng/ml CSF-1 + 50ng/ml FGF-2 + 50ng/ml VEGF (in the case of the vascularized brain organoids (Day 0 of co-culture)

Day 26 iMacs were obtained by transferring the supernatant of Day 26 iMac differentiation plates into a 15ml tube and spinning down at 20^{o}C and 1200rpm for 5min. These cells were resuspended in 1ml ODM+VitA supplemented with 50ng/ml CSF-1 and counted using an Invitrogen™ Countess™ Automated cell counter. Lastly, 150,000

iMacs were seeded into each well of the 24-well plate containing the organoids and the plate was left undisturbed for 4 days. On the fifth day and thereafter on every third day, the media in the 24-well plate was half-replaced while ensuring the prevention of any cross-contamination between the co-cultured and non-co-cultured wells. The non-co-cultured wells were grown identically to the co-cultured ones with the exception that no cells were added on Day 0 of co-culture. Both sets of organoids were imaged using the 4x objective under trans illumination on an EVOS FL Auto system every 4 days. The organoids were co-cultured for 18-28 days with the exact duration of co-culture determined by visual changes in the size of the organoid.

2.3.8 Organoid Fixation and Sectioning

The Organoids were washed 3x with cold PBS and fixed in 4% PFA overnight at 4^{o}C. The next day, they were washed 3x for 10 min each with cold PBS and then transferred to a 30% sucrose solution where they were left overnight at 4^{o}C. The organoids were then embedded in OCT (Optimal Cutting Temperature) medium which was frozen rapidly using dry ice. The frozen block of OCT was then stored at -80^{o}C until sectioning. The embedded organoids were cut into 18um sections using a Leica cryostat and stuck onto Fisherbrand™ Superfrost™ Plus Microscope Slides. These can be stored at -80^{o}C until IHC staining.

2.3.9 Immunohistochemistry sample preparation

The organoid sections on Superfrost slides were first equilibrated in RT PBS for 20min. They were then blocked with a blocking buffer consisting of 0.5% Triton X-100 and 1% Donkey serum in PBS for 1hr at RT. After blocking, the sections were stained using the desired primary antibodies in PBS containing 1% Donkey serum for 24hrs at 4^{o}C. The next day, the sections were washed 3x with PBS - each wash lasting 10min. They were then incubated with the corresponding secondary antibodies in PBS containing 1% Donkey serum overnight at 4^{o}C. The next day, the sections were stained with DAPI (ThermoFischer, #62248) at RT for 1hr in PBS containing 1% Donkey serum. After washing the sections 3x in PBS at RT, they were embedded in the mounting medium

(Abcam, ab128982) for further analysis by confocal microscopy using an FV1000 or FV3000 confocal microscope (Olympus, Japan) and analysed using the Imaris software (Bitplane, Switzerland).

2.3.10 Flow cytometry sample preparation

A single-cell suspension was prepared from the brain/ fusion organoids by treatment with Accutase for 15min at 37°C accompanied by mechanical disruption using a P1000 pipette and rapid trituration every 5min. For cells already in suspension (iMacs), this step was performed for 5min only. The Accutase was then inactivated using FACSBuffer and the cells were spun down at 250-300g for 5min at RT. Following this, the cells were resuspended in the FACSBuffer and stained with the desired antibodies for 20min at 4°C. The cells were then washed and resuspended in FACSBuffer and subjected to Live/Dead staining using DAPI for 5min before acquisition using BD FACSymphony A3 (BD, USA) and analysed on the machine with BD FACSDiva (BD, USA). Following acquisition, the analysis of the flow cytometry data was performed using BD FlowJo (BD, USA)

3. Results

3.1 Human iPSC maintenance and ensuring colony health

It is important when working with hiPSCs to ensure that the cells are healthy and show very minimal differentiation. Although staining with pluripotency markers is a fool-proof method to verify culture quality, it is time-consuming and labour-intensive. As a result, a daily inspection of certain morphological signs under a light microscope is absolutely essential when working with hiPSCs.

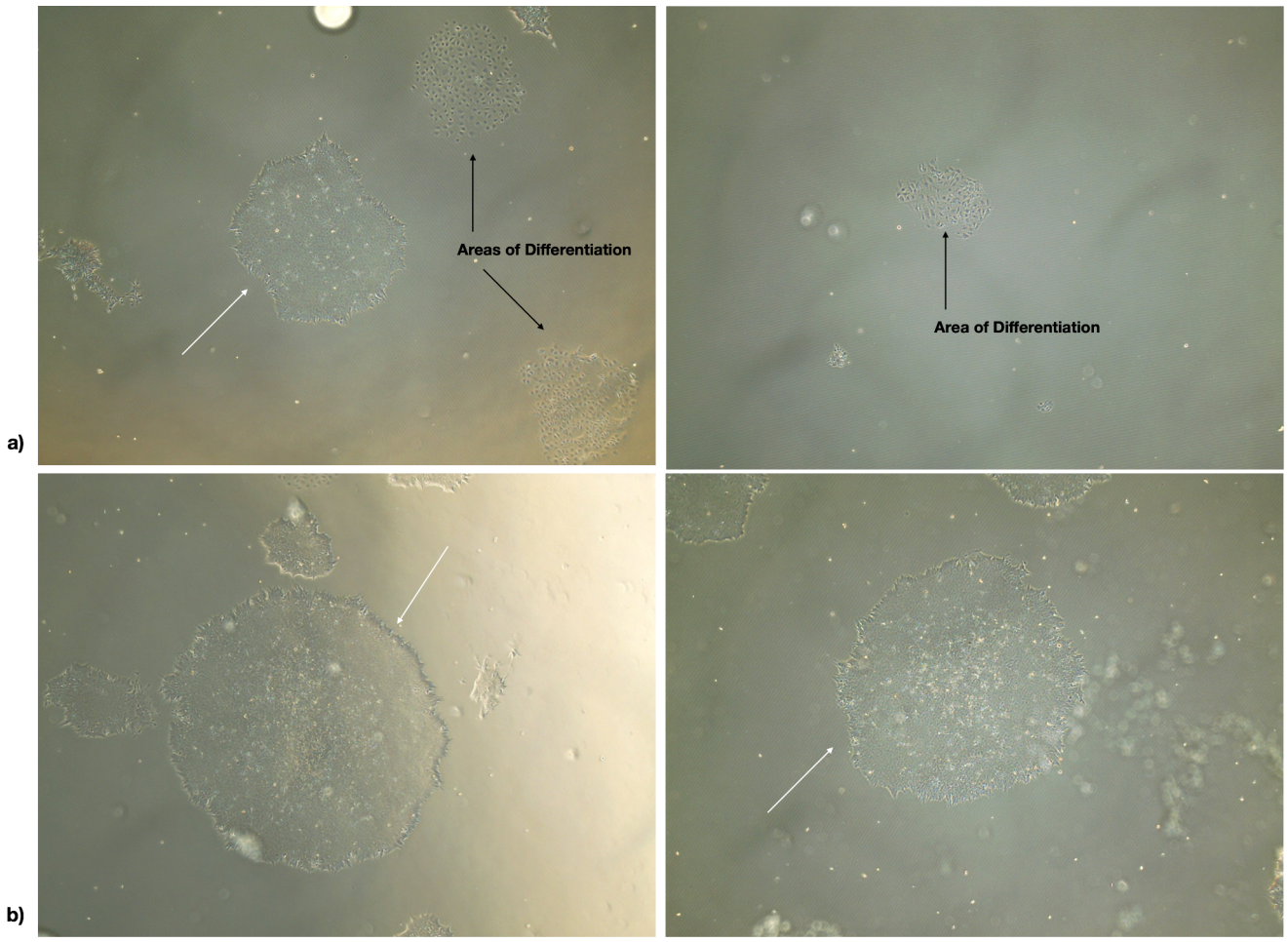

Fig. 3.1: Morphological identification of iPSC colony health and identification of areas of differentiation. a) White arrow shows a healthy iPSC colony next two regions of differentiation (black arrow) in the left panel and a singular differentiated colony in the right panel. b) White arrows show healthy iPSC colonies showing minimal differentiation and a multilayered centre.

Healthy iPSCs form densely packed colonies which are multi-layered near the centre (indicated by brightening under a phase contrast microscope) and display smooth edges (Fig. 3.1a). Looking at individual cells under a higher magnification shows large prominent nucleoli which is a characteristic of hiPSCs. The cells should be passaged when the colonies just touch one another as early or late passaging can lead to signs of differentiation. Differentiated cells typically appear around the edges of large iPSC colonies identifiable by an increase in cell volume as well as by a “spiky” appearance of the colony boundary. Differentiated cell colonies display loose packing and irregular colony shape (Fig. 3.1b).

In all the cultures used in this report, the extent of differentiation was < 5% before seeding cells for Brain organoids, blood vessel organoids, or iMicros.

3.2 iPSC-derived brain organoids

To study the effect of blood vessels on neuronal differentiation as well as the interactions between iMicroglia-blood vessel interactions, it was first necessary to establish a 3D *in vitro* environment which recapitulated the developing neuroectoderm. Towards this end, we used a modified version of the protocol by Lancaster et al. which has been established in the lab (Fig. 3.2a) (Lancaster and Knoblich, 2014). The organoids were seeded on Day 0 and successful progress of differentiation was ensured by monitoring the organoid every alternate day (Fig. 3.2b). Two days after seeding, the aggregates showed a uniform dark structure with clearly defined boundaries. Dead cells were scattered around the aggregate and these did not cause any further problems during the differentiation. Four to five days after seeding, the aggregates began to show signs of brightening (Fig. 3.2b, Day 4) and measured ~400μm in diameter (Fig. 3.2c). This observation was seen to be essential in successful Brain organoid differentiation as failed organoids showed rough edges or large sizes combined with high cell density. When these organoids measured ~600μm (around Day 6) they were transferred into the Neural Induction Medium (NIM) which only supported ectodermal growth. Two days after neural induction, the aggregates showed a size increase in the NIM, had smooth edges, and a brightening around the periphery with a dense core (Fig. 3.2b; Day 8). This observation was seen to be most consequential in ensuring successful brain organoid differentiation as aggregates exhibiting rough dying

edges, a lack of growth in NIM, and the absence of the bright ring surrounding the dense core showed fragmentation at later time points and did not survive. Once this bright ring was visible, the organoids were grown for an additional 2-4 days until a radial organization, characteristic of the neuroectoderm, around the periphery, was evident.

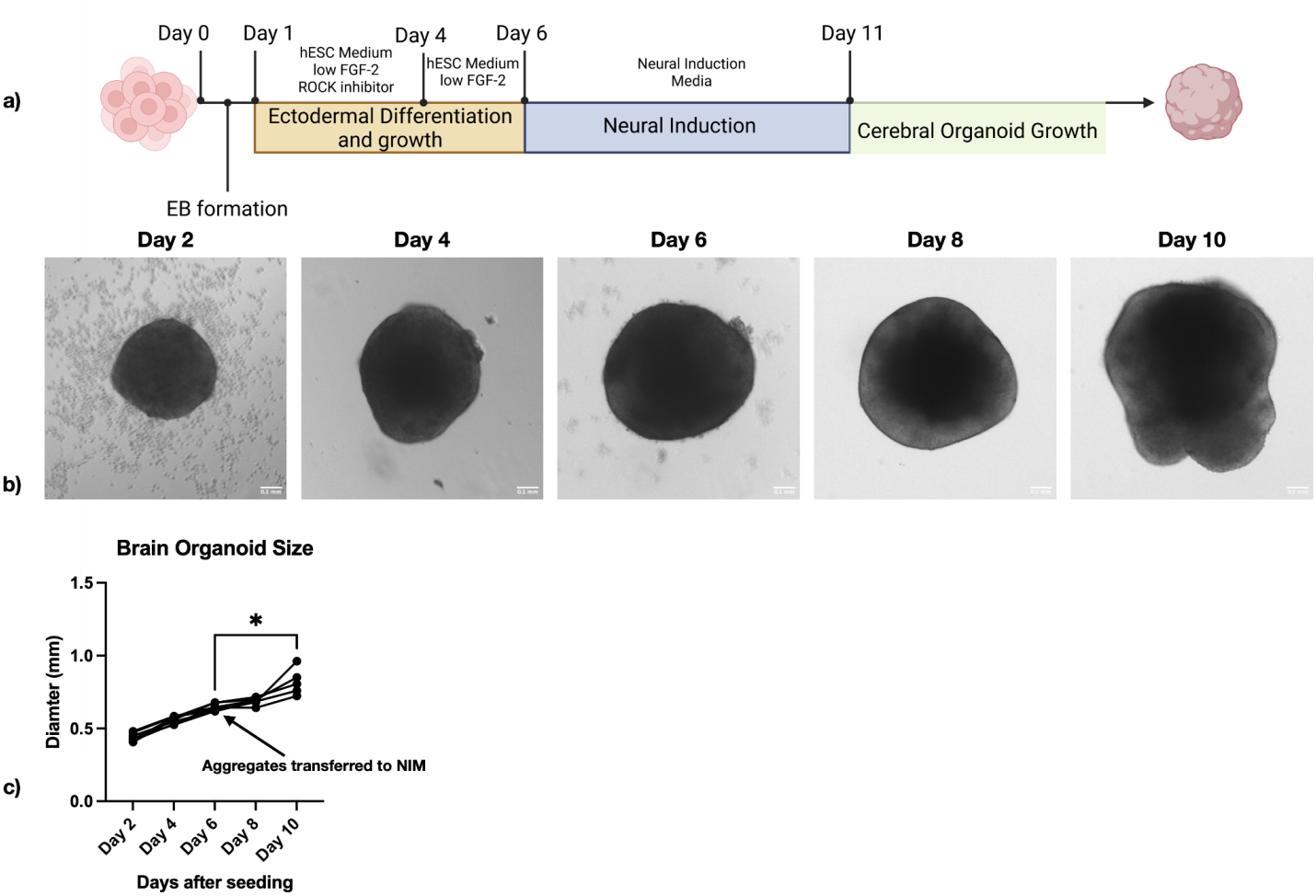

Fig. 3.2: Differentiation of hiPSCs into Brain Organoids. a) Schematic of the protocol for differentiation of hiPSCs into brain organoids. b) Morphological features of the brain organoids during the course of differentiation. Observe the brightening of the organoid around Day 4-6 and the bright ring of Neuroectoderm around Day 8 (Scale bar = 0.1mm). c) Changes in the size of brain organoids along the course of differentiation (7 replicates). Organoids are transferred to NIM at Day 6 when they are ~600µm in diameter.

After embedding the aggregate in matrigel, they were grown for five more weeks before the identification of constituent cell types using flow cytometry. It is important to let the organoids grow for this duration to ensure sufficient diversity of cell types is visible confirming the proper course of differentiation (Fig. 3.3). We observed the generation of a predominantly $CD14^{-}CD45^{-}$ non-haematopoietic population which further indicated the absence of any innately generated microglia ($CD14^{+}CD45^{+}$) in the brain organoids.

This emphasises the absence of an immune compartment in the organoids in the absence of externally introduced iMicroglia as well as in the absence of the necessary growth factors. Gating on the $CD14^{-}CD45^{-}$ population, identified three subsets of cells described as $CXCR4^{+}CD44^{+}$ Glial (astrocyte-restricted) progenitors, $CXCR4^{+}CD44^{-}CD24^{+}CD271^{-}$ Neural Progenitor Cells (NPCs), and $CXCR4^{-}CD44^{-}CD24^{+}CD15^{-}$ Neurons. CD44 was identified in the literature to be a marker for astrocyte-restricted progenitors, and its absence indicates a population of cells capable of or exhibiting neuronal differentiation ((Liu *et al.*, 2004)CXCR4 identifies neural progenitor cells and early neurons with the marker being turned off as the neurons mature illustrating its use for separating the NPC and mature neuron populations.

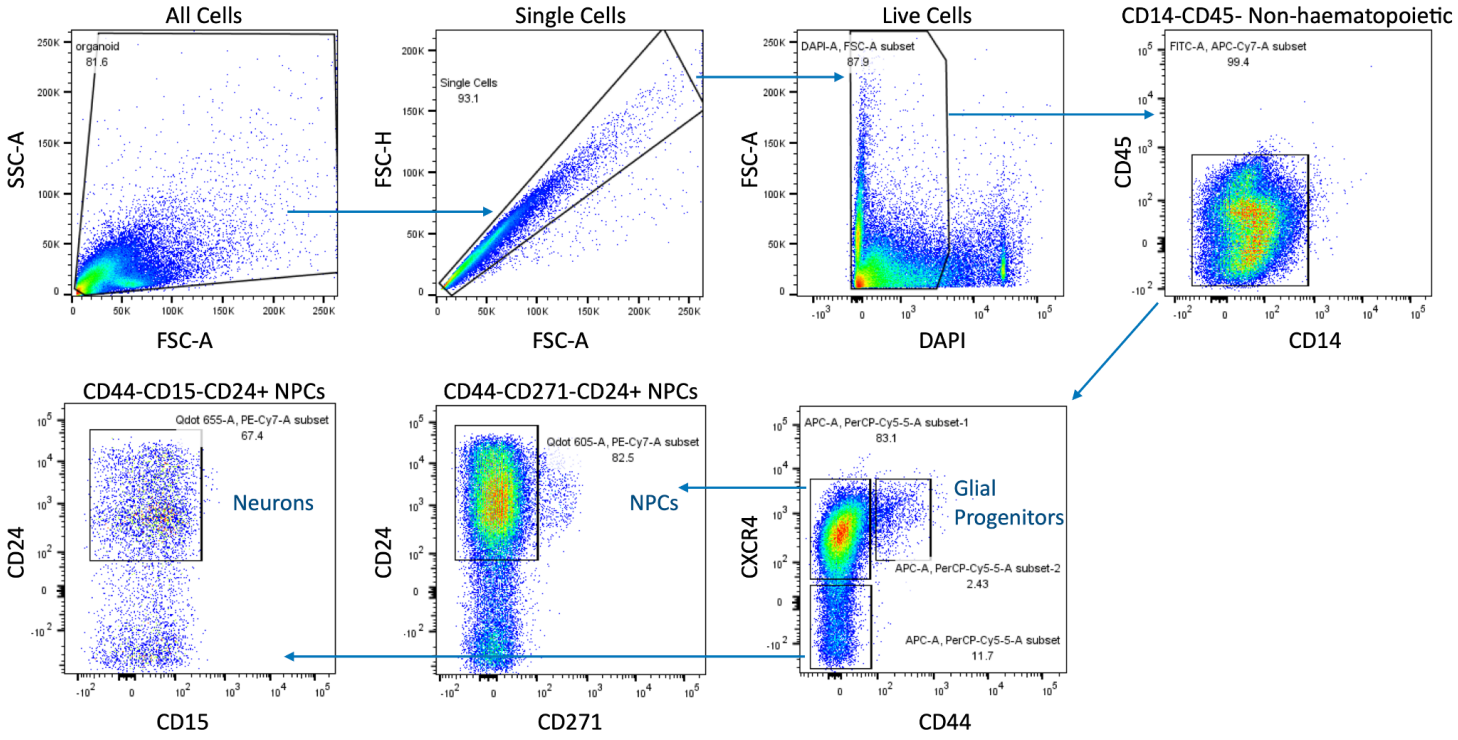

Fig. 3.3: Gating strategy for identification of the different CNS cell types seen in the developing brain organoid at 44 days after seeding. After gating for $CD14^{-}CD45^{-}$ non-haematopoietic cells, we observed the presence of Neural progenitors - the dominant subset at this time point, neurons, as well as a smaller population of glial (astrocyte) progenitors.

Lastly, CD15 is used to gate out myeloid cell populations and CD271 is used to gate out contaminating Neural Crest Cells of the mesodermal lineage in the NPC population (Gadhoum and Sackstein, 2008; Bowles *et al.*, 2019). In addition to the information obtainable by flow, immunohistochemistry images of brain organoid sections reveal the

appropriate spatial localization of neural progenitor cells into rosettes as seen *in vivo* (Fig. 3.12a)

In order to ensure the neurons generated in the brain organoid were actually functional, we also investigated their ability to form synapses with other neurons. Staining of the presynaptic marker PSD95 (Fig. 3.4, left panel) and the post-synaptic marker vGLUT1 (Fig. 3.4, centre panel) showed colocalization between the pre-and post-synaptic markers (Fig. 3.4, right panel; overlay, yellow) indicative of synapses.

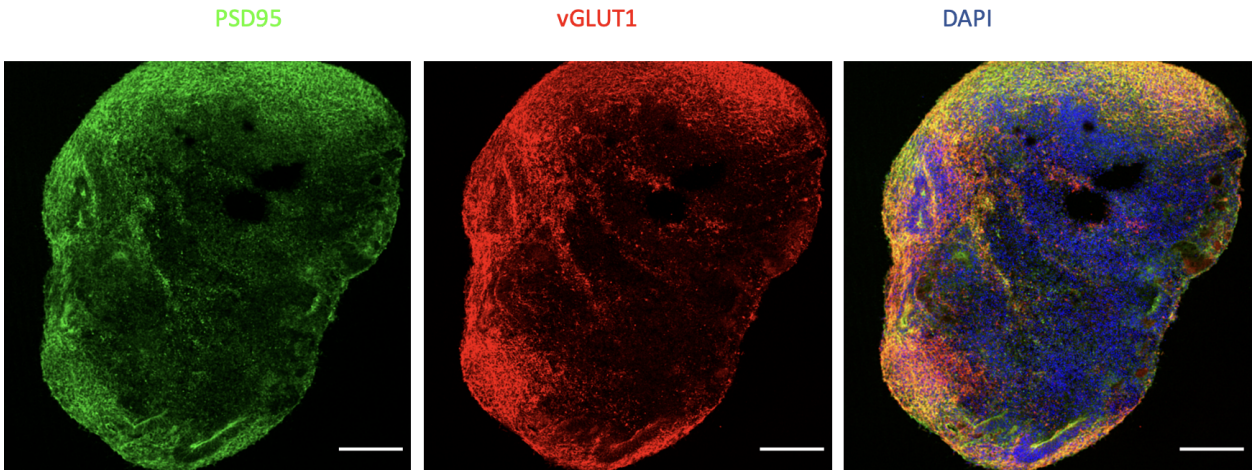

Fig. 3.4: Observation of Neuronal Synapses in Day 44 Brain Organoids. Staining for the presynaptic marker PSD95 and post-synaptic marker vGLUT1 shows the formation of synapses between neurons in the developing brain organoids emphasising the functionality of the iPSC-derived neurons. Scale bar = 0.3mm (Images acquired by Dr. Satish Kumar Tiwari, Post Doctoral fellow - FG Lab, SIgN)

We also tested another brain organoid protocol which utilised the Dual-SMAD inhibition approach to generate brain organoids with a more cortical identity (Fig. 3.5a) (Sun *et al.*, 2022). Although we initially observed the proper progression of differentiation indicated by similar proportions of cells seen via flow cytometry (Fig. 3.5b), later observations around two months after seeding indicated excessive neuronal differentiation at the cost of the NPC population. Furthermore, these two-month-old organoids showed a breakdown in the NPC orientation and organization (Fig. 3.5c). As we could not identify the reason for this difference between the two protocols, we discontinued the use of these Dual-SMAD inhibition organoids for further fusion and characterization.

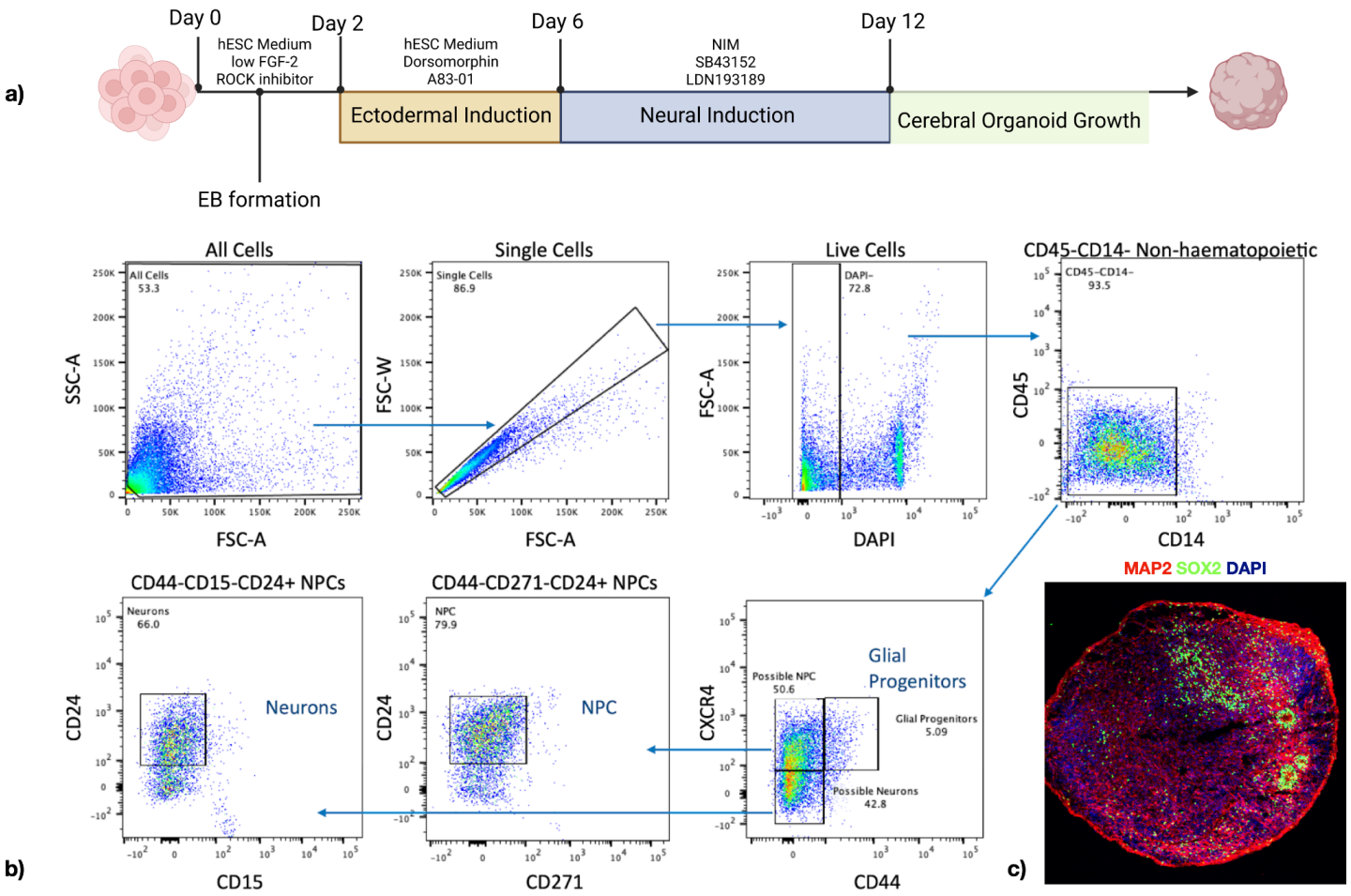

Fig. 3.5: Differentiation of hiPSCs into Brain Organoids using Dual-SMAD inhibition. a) Schematic of the protocol used to generate brain organoids of cortical identity from hiPSCs using Dual-SMAD inhibition. b) Gating strategy for the verification of CNS cell diversity in Dual-SMAD brain organoids. c) Observation of excessive neuronal differentiation (Neuron, MAP2$^+$)(ubiquitous staining in the red channel) and breakdown of progenitor organization (regions of scattered staining in the green channel) (NPC, SOX2$^+$).

3.3 iPSC-derived Microglia

The absence of innately generated microglia in the brain organoids under normal culture conditions necessitated the introduction of separately differentiated iPSC-derived microglia (iMicros). Towards this end, we used a protocol established in the lab first described by Takata et al. in 2017 (Fig. 3.6a) (Takata *et al.*, 2017). Briefly, iPSCs were plated as small clumps ~50-100μm in diameter on matrigel-coated plates. After successful attachment, they were differentiated into the primitive streak mesoderm by exposure to the GSK-3 inhibitor CHIR99021 and BMP4 under hypoxia. This primitive streak expressed VEGFR-2 (KDR$^+$) and was expanded in the presence of BMP4,

FGF-2, and VEGF. This process was continued for 6 days giving rise to primitive haemogenic endothelium. Observations of cell colonies in this period reveal striking changes after the onset of hypoxia (Fig. 3.6b). Two days into hypoxia, the cells began to display an increased cytoplasmic volume and an elongated shape as well as a loss in iPSC-like colony integrity near the periphery (Fig. 3.6b; left panel, asterisk). On days four to six of differentiation, the cells showed rapid proliferation under hypoxia. The colonies now adopted an island-like appearance with densely packed round cells in the centre and the cells forming a 3D rope-like continuous structure around the boundary (Fig. 3.6b; centre, right panels, arrows). This morphology of cells has previously been associated with primitive yolk sac myelopoiesis in mice (Muffat *et al.*, 2016).

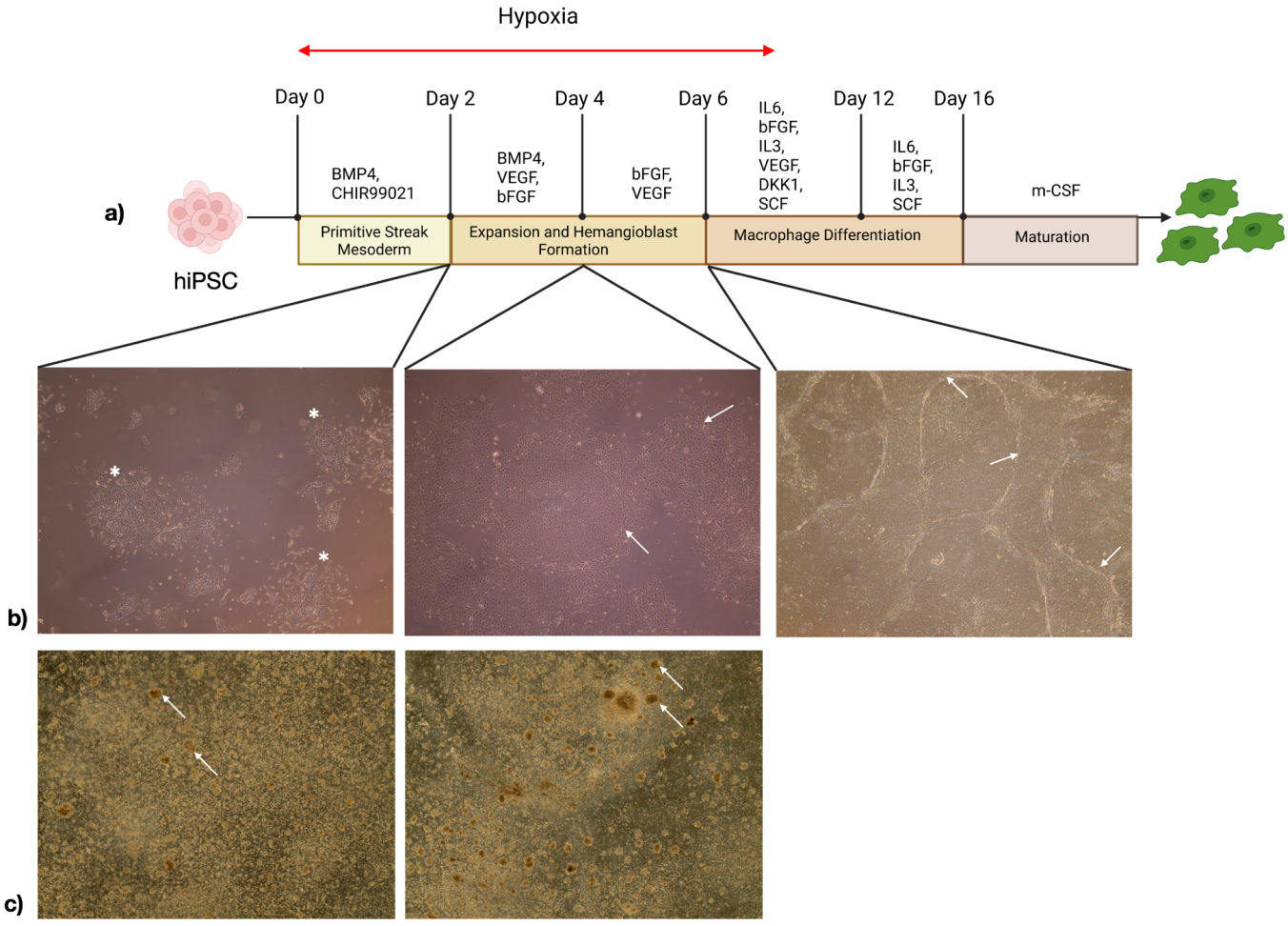

Fig. 3.6: Induced Macrophage (iMac) differentiation of human iPSCs. a) Overview of the protocol for differentiation of hiPSCs into iMacs. The coloured boxes highlight the different developmental stages. b) 4x objective phase contrast image of the plate at the specified time points. (left) The asterisks indicate the first hallmark of differentiation with a breakdown of the densely packed colony boundary. (centre, right) arrows point to the 3D rope-like structures which surround island-like colonies - this morphology is associated with yolk sac myelopoiesis. c) Numerous macrophage clumps are seen on day 22 of iMac differentiation - 6 days after CSF-1 initiation. The arrows indicate the most prominent clumps.

Primitive haematopoiesis was initiated after Day 6 by exposure to haematopoietic cytokines as well as the Wnt antagonist Dickkopf Wnt pathway inhibitor 1 (Dkk1) to pattern away from definitive haematopoiesis. Primitive haematopoiesis was then allowed to proceed for ten more days during which light microscopy observations were of limited utility due to the high cell density. Over time, an increasing number of floating cells began to appear which are thought to be microglial precursors that bud off the surface of the plate. These floating cells were then allowed to mature into primitive yolk sac-like macrophages by exposure to a high concentration of Macrophage Colony Stimulating Factor (CSF-1) for ten more days. Immediately after CSF-1 onset, the floating cells begin to rapidly proliferate as well as aggregate into irregularly shaped floating aggregates - a characteristic of myeloid cells. (Fig. 3.6c; white arrows show the largest aggregates).

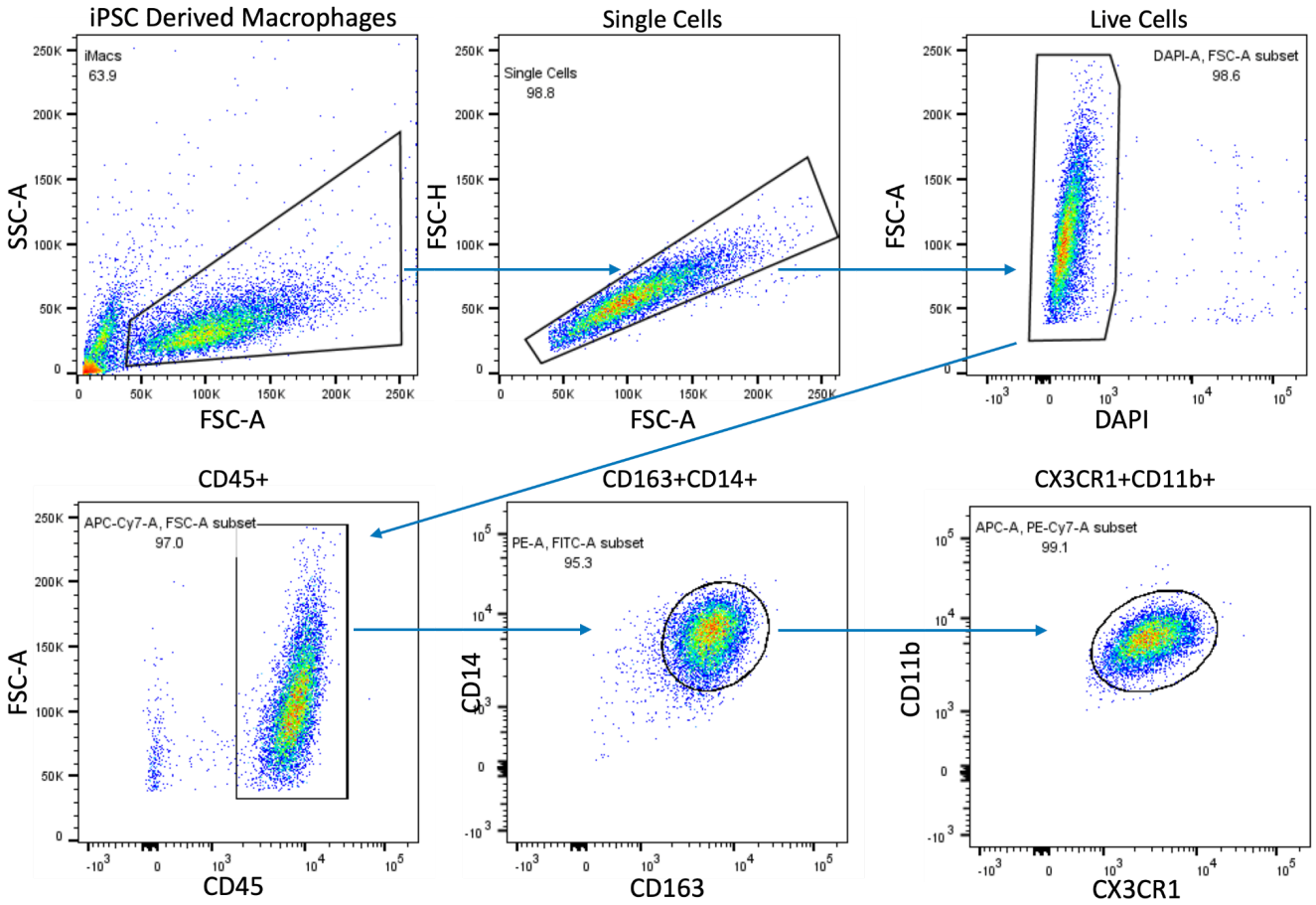

Fig. 3.7: Induced Macrophage (iMac) confirmation using Flow Cytometry. Gating strategy for identification of iPSC-derived primitive macrophages at day 26 of differentiation. The protocol yields over 90% bonafide iMacs on day 26.

Around Day 26 of differentiation, the identity of these cells as primitive yolk sac macrophages (iMac) was confirmed using flow cytometry (2.7). These cells in suspension, stained positive for the haematopoietic cell marker CD45. Gating on the $CD45^{+}$ revealed a predominant population which was positive for the macrophage markers CD11b, CX3CR1, CD14, and CD163 representing over 90% of all the live cells in suspension. The primitive macrophages have (in previous work from the lab) been cultured with iPSC-derived neurons and brain organoids and have been shown to adopt a ramified morphology and a transcriptional signature reminiscent of fetal microglia. As a result, we did not repeat the verification of microglial transcriptional identity in this report. Furthermore, the high purity of the primitive macrophage population eliminated the need for sorting of the floating cell population and we directly utilized them for further co-culture applications.

3.4 hiPSC-derived Blood Vessel Organoids

Numerous strategies have been used in the literature to induce the formation of vessel-like structures in brain organoids. These involve exposure of the brain organoids to high concentrations of vessel-promoting cytokines like VEGF and FGF-2 or mixing in isolated/cultured endothelial cells. The former typically generates a very low-efficiency induction of endothelial cells (Ham *et al.*, 2020). The latter approach does not allow the introduction of blood vessels at biologically relevant time scales, which can possibly cause defects during the course of brain organoid differentiation. As a result, we decided to use a fusion protocol to introduce iPSC-derived blood vessels into the brain organoid similar to *Sun et al.* (Sun *et al.*, 2022).

We first tried a large number of protocols to induce endothelial cells from iPSCs (see Table 1) modified for use in our case on embryoid bodies. These protocols (numbered 1 to 8) utilize a basic pattern, with initial patterning to the mesoderm using different combinations of CHIR99021 and/or BMP4 followed by induction of endothelial cells in the presence of high concentrations of VEGF and/or FGF-2 (except protocol 3 which also uses the adenylyl cyclase activator Forskolin (dissolved in ethanol) - discussed later) - see Fig. 3.8a for a schematic of the protocol by Sun et al. We modified a variety

of parameters during the optimization of these protocols including the size of the aggregate (varied by changing the number of cells seeded/well), duration of induction, and the concentrations as well as combinations of different cytokines used. However, we were unable to induce >3% $CD31^+$ endothelial cells in any of our attempts (Fig. 3.8b, c).

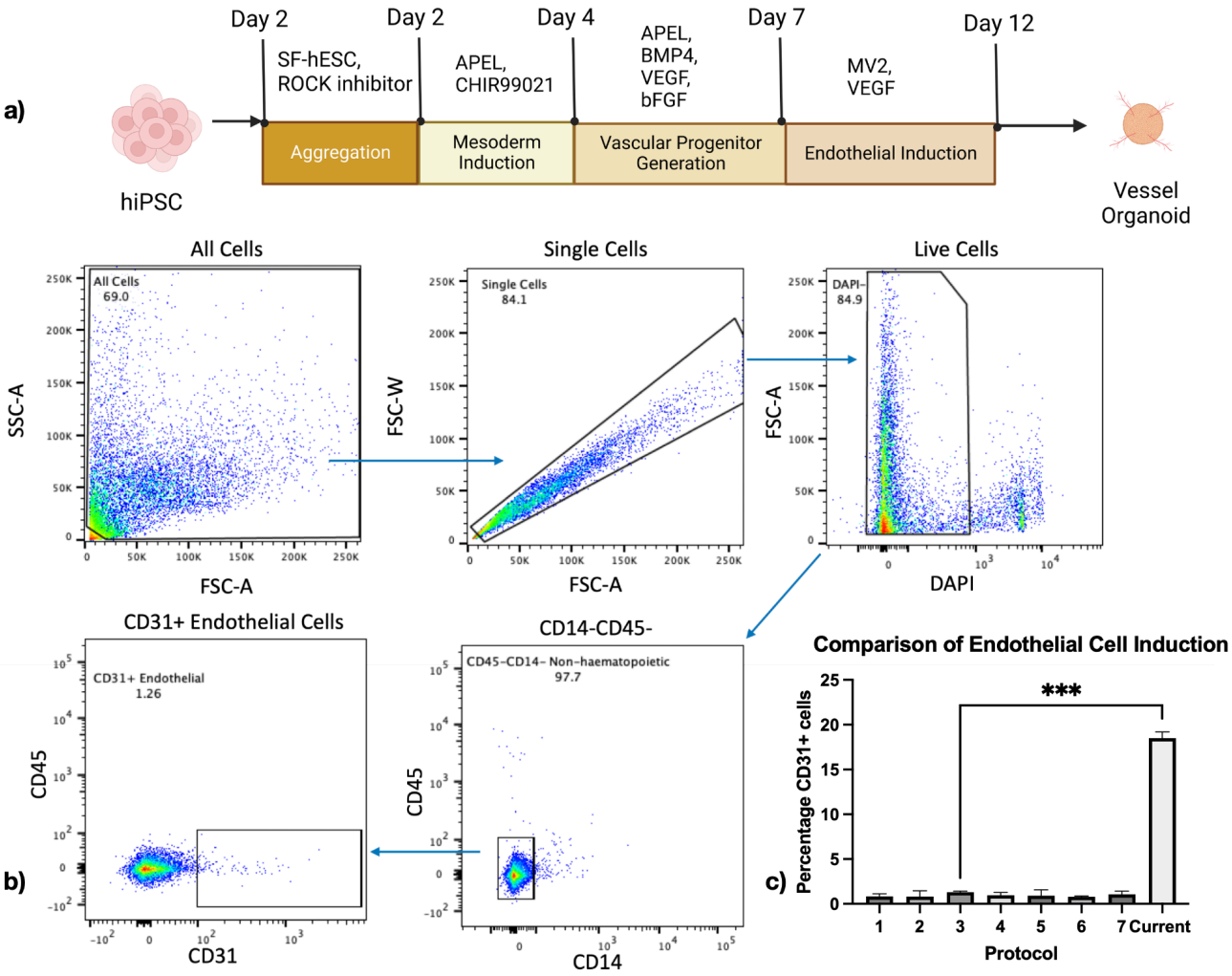

Fig. 3.8: Representative schematic and gating strategy for protocols reported in the literature for the generation of iPSC-derived endothelial cells or blood vessels. a) Schematic representation of the protocol by Sun et al. which also described the general pattern reported in the literature for the generation of iPSC-derived blood vessels/ endothelial cells. b) Gating strategy for the identification of iPSC-derived endothelial cells. c) Comparison of the protocols identified in the literature (1-7) against our optimized protocol used in the later parts of this work and described in Fig. 3.9a. ***p<0.001 See Table 1 in methods for an in-depth comparison of protocols 1-7.

We initially believed that the large sizes of the aggregates we were seeding compromised the efficiency of differentiation by reducing the surface area to volume

ratio essential for sufficient diffusion of the protein patterning cues to the core of the organoid. However, the very low extent of endothelial cell differentiation in protocol 7 which generated much smaller aggregates pointed to the presence of other factors at play. Returning to the failure of protocol 3 which used Forskolin which was stored at -20°C as an aliquot in ethanol. We think a combination of the adenylyl cyclase inhibitory properties of ethanol, as well as the short shelf-life of forskolin in solution, contributed to the ineffective induction of $CD31^{+}$ endothelial cells (Huang *et al.*, 1982).

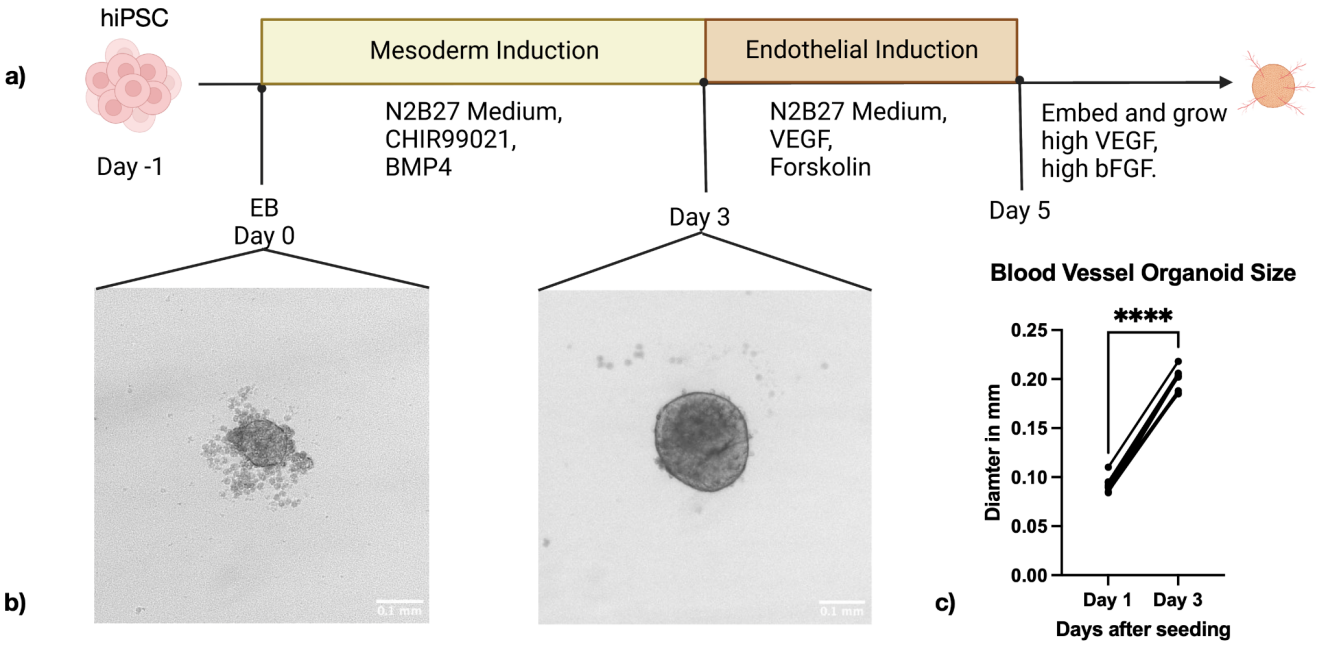

Fig. 3.9: Generation of hiPSC-derived Blood Vessel Organoids using our optimized protocol. a) Schematic of the protocol used for the generation of blood vessel organoids from hiPSCs. b) Images of representative organoids after aggregation (left panel) and after mesoderm induction (right panel). (Scale bar = 0.1mm) c) Changes in the size of the blood vessel organoids along the course of differentiation. Note the highly similar sizes between organoids at corresponding time points.

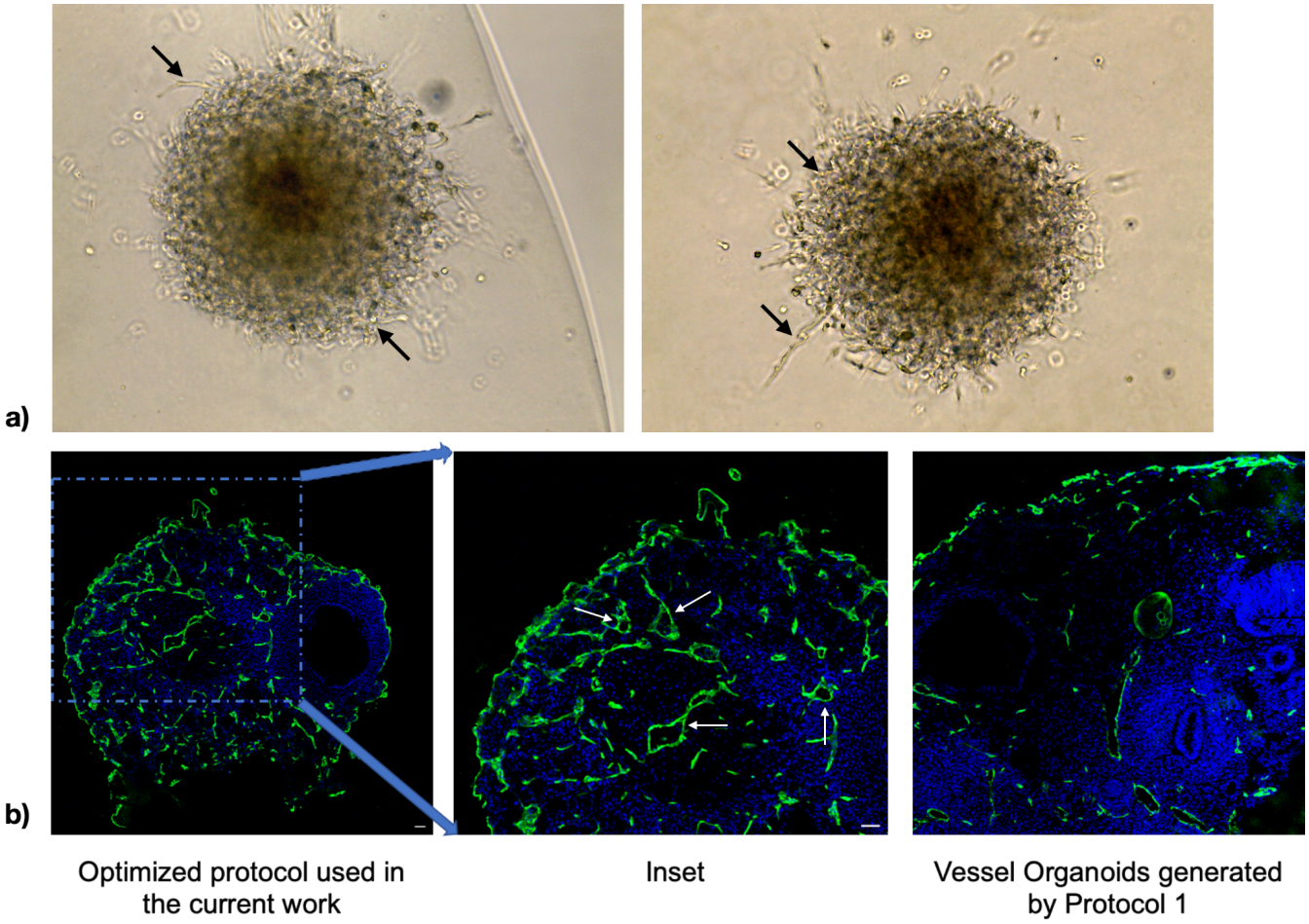

Fig. 3.10: Morphological features seen in the Blood vessel organoids. a) Evidence of extensive sprouting in the vessel organoids seen 3 days after embedding in matrigel (Imaged through 20x objective). b) Comparison by IHC staining of 18um section of fixed and frozen Day 22 vessel organoids stained with DAPI and CD31 (green). A large increase in endothelial cell induction is visible as well as an abundance of vessel-like features (white arrowheads centre panel).

A thorough review of the literature then identified a recent 2019 report by Wimmer et al. which described the development of a protocol for human blood vessel organoids (Wimmer *et al.*, 2019b, 2019a). Furthermore, this protocol claimed to generate $CD31^{+}$ endothelial cells and $CD140b^{+}$ pericytes in a 1:2 ratio which is necessary for endothelial cell survival as well as stable vessel formation. We decided to initially attempt to reproduce their findings in our line of iPSCs as well as investigated the feasibility of adapting the protocol to a 96-well format thereby ensuring greater regularity in the size of the aggregates in a manner similar to Nikolova et al (Fig. 3.9a) (Nikolova *et al.*, 2022). We optimized the number of cells seeded/well to ensure the organoids were between ~50-100µm in diameter after one day of aggregation (Fig. 3.9b, c). After suitably sized aggregates were obtained, we began mesodermal induction using the Wnt agonist CHIR99021 and BMP4 for three days. Observations of the aggregates

showed a uniform brightening of the surface of the organoid accompanied by an increase in size (Fig. 3.9b, c). Lastly, we performed induction of endothelial cells using a new aliquot of Forskolin dissolved in DMSO at 20mM (to minimise DMSO concentrations in solution) and 100ng/ml VEGF. After embedding in matrigel 7 days after seeding, the aggregates showed extensive sprouting away from the core of the organoid which appeared within 2-3 days after embedding (Fig. 3.10a, arrows). Furthermore, immunohistochemistry on 18um sections of frozen blood vessel organoids 22 days after seeding showed visibly higher induction of endothelial cells (Fig. 3.10b, green), as well as the appearance of vessel-like structures (Fig. 3.10b, arrows) as compared to the protocol of *Sun et al.* (Sun *et al.*, 2022).

This was confirmed by flow cytometry using CD31 as a marker for bonafide endothelial cells after gating out all haematopoietic populations as $CD14^{-}CD45^{-}$ (Fig. 3.11a) which also revealed a very significantly higher induction of endothelial cells in our optimized protocol as compared to the ones we tested previously (Fig. 3.8c). Further emphasizing their endothelial cell identity, 60% of the $CD31^{+}$ cells on Day 7 were positive for the late (mature) endothelial cell marker CD144 (VE-cadherin) (Fig. 3.11b).

After we established the protocol for blood vessel organoids in our line of iPSCs we decided to proceed with the generation of fusion-derived vascularized brain organoids using a modified time scale as described in the next section. The high efficiency of differentiation also ensured that confounding results due to rogue regions of differentiation were minimized. Furthermore, the efficiency of vessel generation was high enough to eliminate the need for cell sorting and allowed the use of immunohistochemistry to study the presence of blood vessels after fusion with the brain organoid.

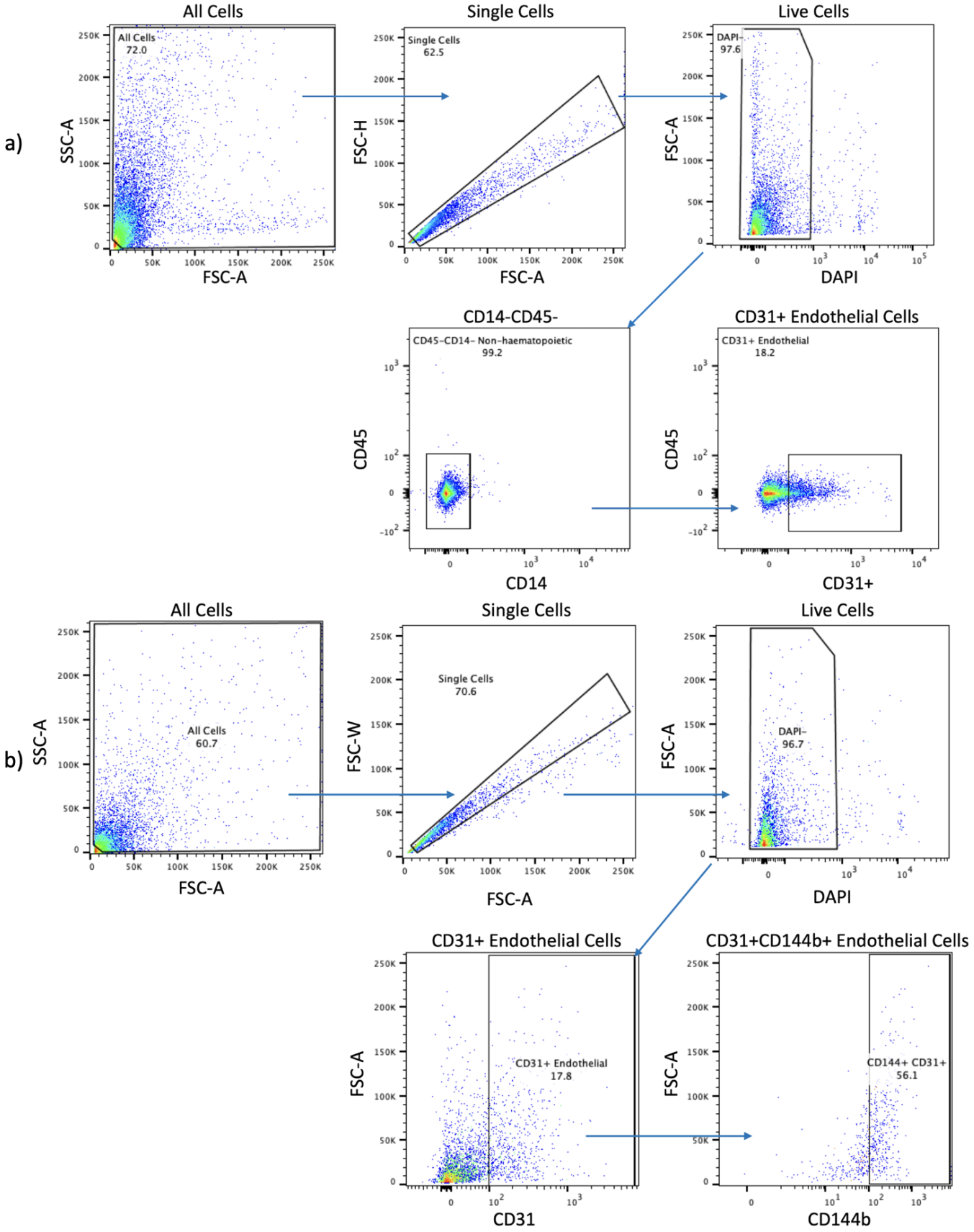

Fig. 3.11: Gating strategy for identification of CD31+ endothelial cells. a) Identification of CD31+ endothelial cells using flow cytometry. Observe the increase in the percentage of CD31+ cells. b) Verification of endothelial cell identity by double staining of CD31 and CD144b (VE-cadherin).

3.5 Fusion Vascularized Brain Organoids

The generation of fused vascularized brain organoids was a significant technical challenge because of the specific conditions necessary for the generation of blood vessel organoids. Our original fusion strategy (based on *Sun et al.*), involved the deposition of a brain organoid and two blood vessel organoids on an organoid embedding sheet followed by residual media aspiration and deposition of a matrigel droplet. However, due to the extreme sensitivity of endothelial cell induction to the size of the aggregate, our vessel organoids were just ~100µm during embedding. This meant that they weren't visible during media aspiration and positioning them around the brain organoid with a pipette tip was impossible. After multiple attempts, we settled on the workflow described in Fig. 3.12a which allowed us to generate ~12-15 matrigel droplets containing one brain as well as 3-4 vessel organoids within 30 minutes. The number of embedded vessel organoids per droplet was increased owing to their smaller size and the short time scale was essential to maintain the integrity of the matrigel droplets.

In addition to the technical difficulties, we had to stagger the seeding of the brain and vessel organoids to ensure that they were ready on the appropriate day for fusion (Fig. 3.12b). After embedding, the matrigel droplets were incubated in ODM-VitA for four days followed by ODM+VitA until the analysis time point - both supplemented with 100ng/ml VEGF and 100ng/ml FGF-2. Within 2-3 days after embedding, excessive sprouting was seen from the vessel organoids with minimal sprouting from the larger brain organoid (Fig. 3.12c).

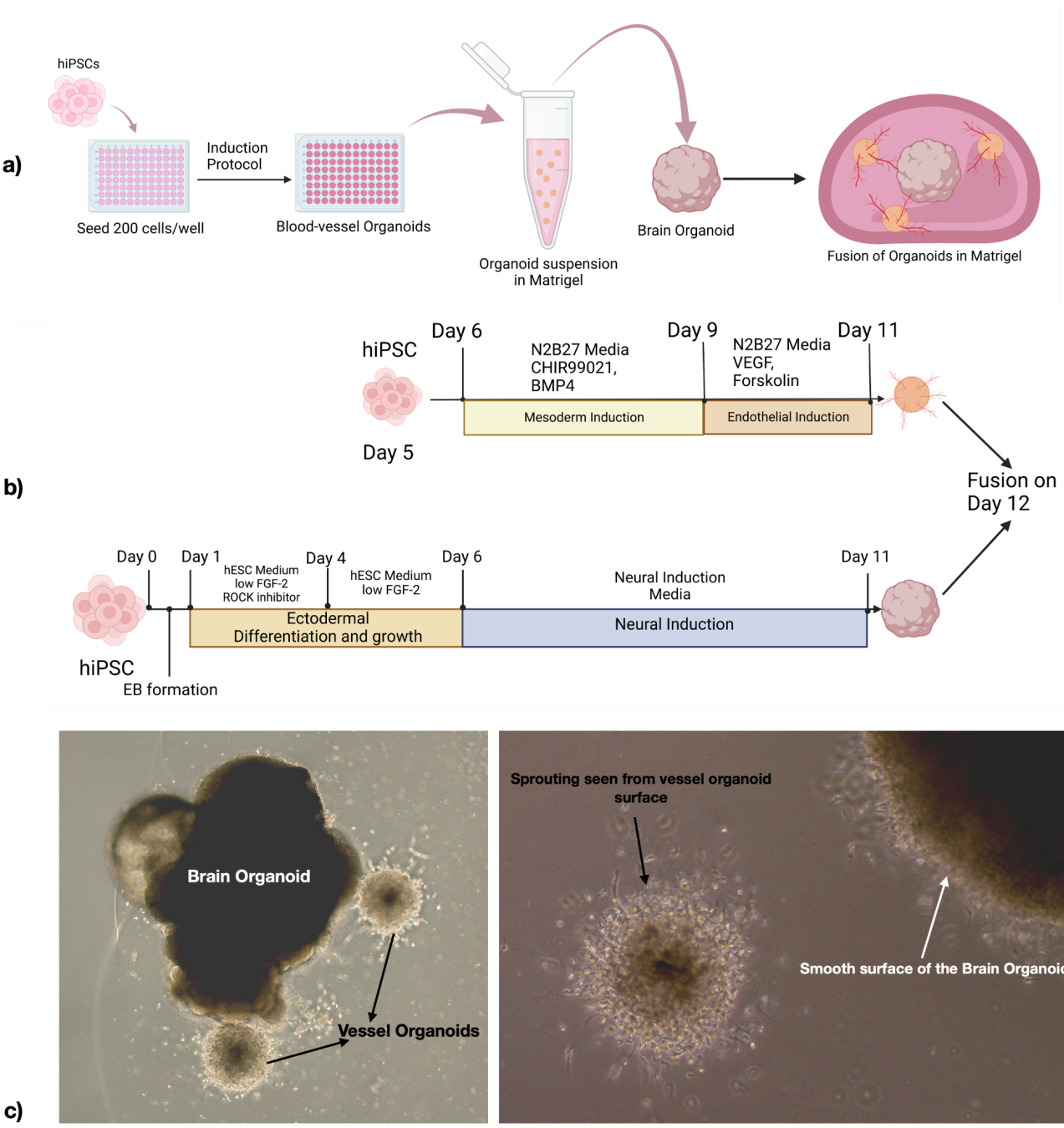

Fig. 3.12: Fusion of iPSC-derived blood vessel and brain organoids and the generation of fused vascularized brain organoids: a) Workflow for the co-embedding iPSC-derived brain and vessel organoids in one matrigel droplet. b) Schematic of the protocol used in the generation of fused vascularized brain organoids. c) Phase contrast microscopy images of the co-embedded organoids in matrigel three days after embedding. Left Panel, 4x objective;. Right Panel, 10x objective; observe extensive sprouting from the surface of the blood vessel organoid and the relatively smooth surface of the brain organoid.

The fusion organoids (FVOs) were allowed to grow for two weeks after embedding before they were used for co-culture experiments or sacrificed for analysis. Two main

methods of analysis could be used at this stage - flow cytometry and immunohistochemistry of fixed frozen sections. Due to the small size of the organoids on Day 26 as well as our limited batch size, we chose not to perform a flow cytometric characterization. Instead, two FVOs were fixed in PFA and frozen in a block of OCT (optimal cutting temperature) compound for sectioning. 18um thick sections of the organoids were then stained with makers for Neural Progenitors (NPC; SOX2, green), Neurons (MAP2, magenta), and Endothelial Cells (CD31, Red) along with DAPI to stain cell nuclei (Fig. 3.13a, b).

An observation of the SOX2 staining reveals an abundant population of NPCs in line with the dominant progenitor population at this early developmental time point (approximately 4 weeks *in vivo).* Furthermore, the NPCs appear to orient themselves into regions of radial organization reminiscent of the Neural Rosettes seen during development *in vivo* and in other brain organoid differentiation protocols (Fig. 3.13a, arrow) ((Lancaster *et al.*, 2013)The proper orientation of progenitor zones emphasised the robustness of the ongoing neurodevelopmental programs even in the presence of a high concentration of VEGF and FGF-2. Furthermore, MAP2 staining (which stains both neurons and NPCs - the filamentous projections label neurons typically going radially outward from the rosette) revealed regions of neuron formation revealing the early stages of neurogenesis from the NPCs. The presence of NPCs and neurons in the organoid as well as no overtly visible structural disruptions in the brain organoid progenitor organization minimised the possibility of rogue endothelial cell differentiation and vessel formation within the brain organoid.

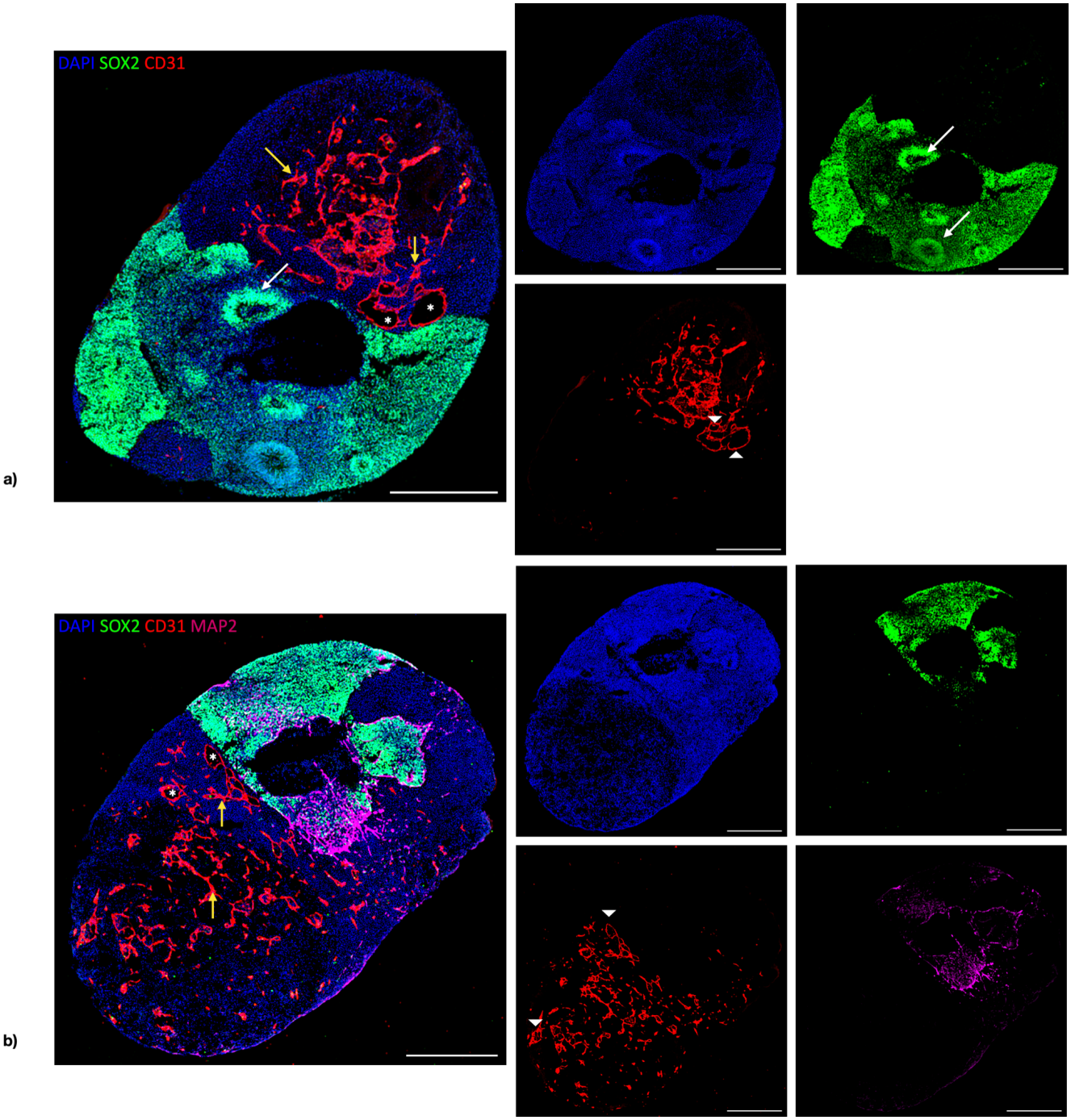

Fig. 3.13: Immunohistochemistry images of fixed and frozen 18um cryosections of fused vascularized brain organoids. a,b) Staining of the sections with markers for NPC (SOX2, green), Neurons (MAP2, magenta), Endothelial cells (CD31, red), and Nuclei (DAPI, blue) reveals abundant induction of endothelial cells and formation of branching blood vessels (white asterisks, white arrowheads, and yellow arrows) in close apposition with CNS cell types including NPCs and Neurons. (White arrows locate Neural Rosettes which are also seen during *in vivo* neurogenesis). The two sections belong to two different fused organoids. (scale bar = 0.5mm)

More consequential to this work, however, is the staining in the CD31 channel (red). CD31 marks cell junctions between endothelial cells and is hence strongest where the vessels branch or fuse. In addition to the strong staining, a halo of CD31 is observed at non-membranous regions. The red channel shows a large number of vessel-like structures (seen as circles in section, 2.13a,b; arrowhead) with empty lumens (seen by the absence of DAPI staining in the lumen, 2.13a,b; asterisk) and show multiple bright branching points (2.13a,b; yellow arrowhead). Some of these vessels appear as lines of CD31 staining as they were sliced longitudinally along their lengths while others show circular lumens. Furthermore, emphasising the utility of this model system, the vessels are seen in close apposition with the brain organoid allowing for contact as well as cytokine-mediated interactions between the blood vessels and NPCs/ neurons. Furthermore, no large-scale morphological features were visible (other than the vessels and structures in the brain organoid) lending support to the idea that off-target differentiation in the system as a whole was minimal.

Once we had established a protocol and workflow for the generation of vascularized brain organoids and confirmed the above-described structural features and maintenance of iPSC-derived endothelial cells over long culture durations, we moved on to the introduction of iMacs (which differentiate in the organoid into iMicros) into the fusion-derived vascularized brain organoids to explore their effect on the different cell population seen in the FVOs.

3.6 Co-culture of Fusion organoids with iPSC-derived Primitive Macrophages

A few different strategies exist in the literature for the incorporation of microglia into the developing brain organoids. They typically involve the addition of microglial precursors in the cell suspension while seeding the organoid or *in vivo* transplantation of the organoid in mice. However, the entry of microglia into the developing neuroectoderm in humans is very tightly controlled and the temporal dynamics of microglia are necessary for certain developmental events (Hattori *et al.*, 2020). As a result, premature incorporation of microglia could lead to developmental defects. The *in vivo*

transplantation approach does not allow the incorporation of human microglia and requires sophisticated surgical expertise. We decided to exploit the migratory nature of iMacs and used a co-culture strategy for the introduction of hiPSC-derived microglia (iMicros) into the brain organoid at a biologically relevant time point (Fig. 3.14a).

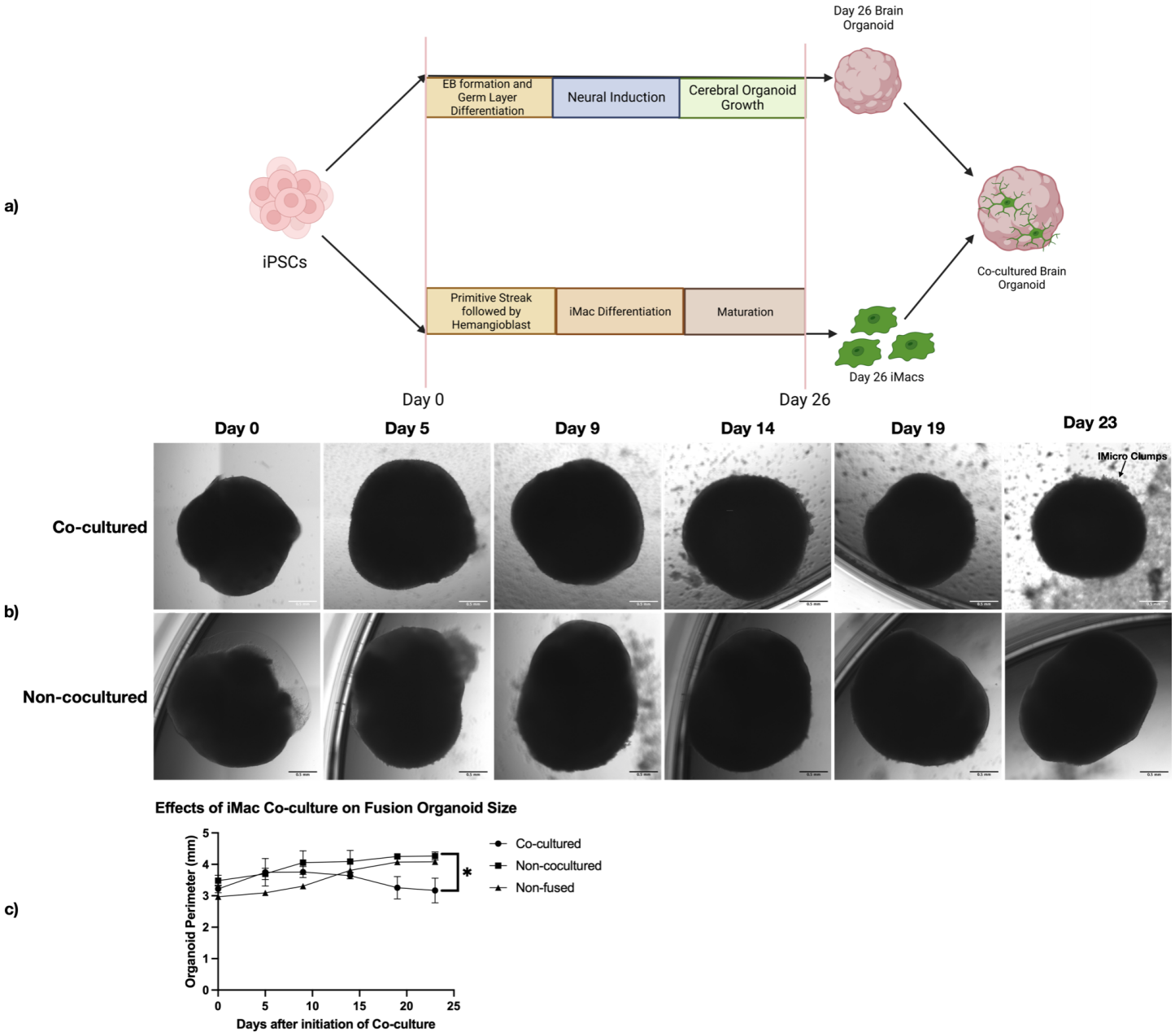

Fig. 3.14: Co-culture of Fusion Vascularized Brain Organoids with iPSC-derived primitive macrophages. a) Schematic of the protocol and the timeline used to co-culture Fusion Vascularized Brain Organoids and iMacs. b) Observation of organoid morphology along the course of co-culture for both co-cultured and non-co-cultured organoids. Observe iMicro clumps on the surface of late co-cultured organoids (After Day 14). (Scale bar = 0.5mm). c) Changes in organoid size along the duration of co-culture. (*p<0.05)

Day 26 after seeding of the brain organoids was chosen as the start date for co-culture as the organoids at this stage exhibit a developmental state similar to that seen around 4.5 weeks post-conception when microglia first appear in the developing human brain (unpublished work from the lab). At this time point, the brain organoids or fusion organoids were transferred into 24-well ultra-low attachment plates with 150,000 iMacs per co-cultured well and grown in ODM+VitA. The media was supplemented with CSF-1 and in the case of the fusion organoids, additionally supplemented with VEGF and FGF-2. Observations of organoid size every three days revealed a curious decrease in the size of the co-cultured organoids as compared to the ones grown under similar conditions in the absence of iMacs (Fig. 3.14b). This decrease in organoid size is further described in recent work from the lab and will not be discussed further here.

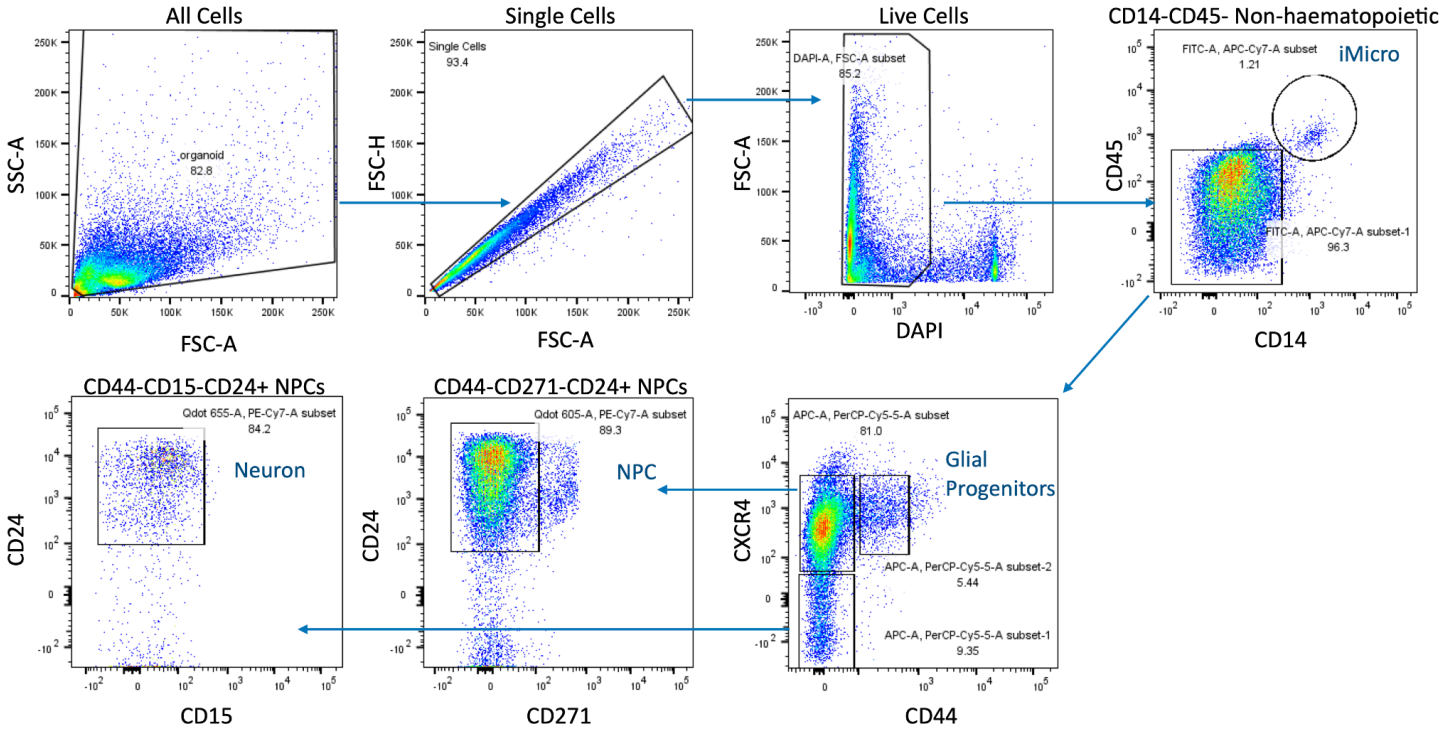

Fig. 3.15: Gating strategy for co-cultured Brain Organoids. The figure shows the gating strategy used for the identification of the diversity in differentiated cell types in Day 54 co-cultured brain organoids. Observe the small cluster of $CD45^{+}CD14^{+}$ double positive iMicros.

The organoids were co-cultured for 18 to 28 days and analysed at the endpoint using flow cytometry. As we were only able to generate a small batch of organoids until now due to the requirement for extensive standardization and optimization, we were unable to perform both flow cytometry and immunohistochemistry. At this time point, we wished

to ensure the appropriate generation of a variety of CNS cell subtypes and decided to perform a flow cytometric characterization using the panel described in Fig. 3.3a combined with staining for the endothelial cell marker CD31. Before looking at the flow panel for the vascularized organoids, it is instructive to look at co-cultured brain organoids (Fig. 3.15). Three things appear most obvious in this panel. Firstly, the existence of a $CD14^{+}CD45^{+}$ double positive cluster which are the iMicros. Secondly, the population of glial progenitors shows an increase, and thirdly the population in the Neuron gate appears cleaner with a greater proportion of $CD24^{+}$ cells (See recent work from the lab for an in-depth discussion on these observations). These observations are reminiscent of increased maturation in the co-cultured brain organoids.

The flow panel of non-co-cultured fusion organoids (Fig. 3.16a) highlights the presence of around 1% $CD31^{+}$ endothelial cells - a small but expected value owing to the much larger size of the brain organoids. As each flow (non-co-cultured and co-cultured) was performed with one fusion organoid, I will refrain from making any comments about the individual proportions of CNS cell types or differences in differentiation as that will definitely require an analysis of at least 3 organoids of each type. The co-cultured organoid (Fig. 3.16b) shows a small cluster of $CD14^{+}CD45^{+}$ iMicros and more interestingly shows a higher proportion (6%) of $CD31^{+}$ endothelial cells. Although this observation is in line with our hypothesis of a vasculogenic role of iMicros owing to the hypoxic environment in the core of the organoid, a much larger batch of organoids needs to be made to confirm these speculations. At this stage, the only conclusions we draw from the flow panels are regarding the presence and stable maintenance of an observable number of endothelial even after the long 5-week culture duration and a possible increasing trend in the proliferation/ proportion of endothelial cells in the fusion vascularized organoids due to interactions with the co-cultured microglia.

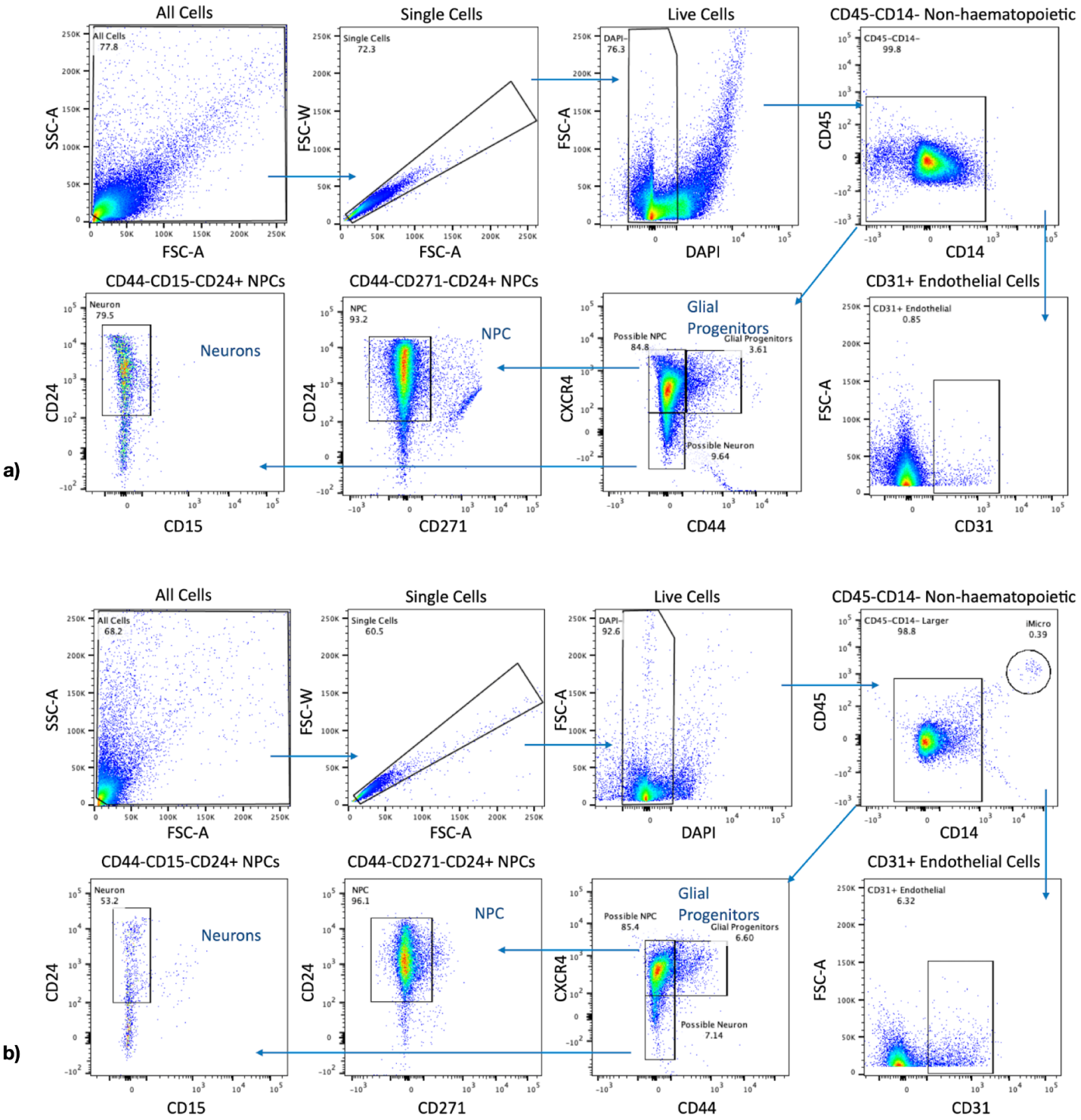

Fig. 3.16: Gating strategy for co-cultured Fusion Vascularized Brain Organoids. a,b) The gating strategy used for the identification of the diverse CNS cell types in addition to the iMicros and CD31^{+} Endothelial cells in the Fusion Vascularized Brain Organoids on Day 56 after seeding. Note the small cluster of iMicros as well as the higher proportion of CD31^{+} endothelial cells in the co-cultured organoid. Each flow is performed using one organoid.

4. Discussion

Microglia specifically and macrophages, in general, have often been attributed to the simplistic role of tissue sentinels. They are present in a “homeostatic” state in the tissues and respond to cell debris or foreign antigens as first responders. This relatively non-specialized role has also resulted in the collective grouping of monocytes and macrophages. For many years, this understanding made discussions of macrophage ontogeny redundant as it was thought they all came from the bone marrow. Furthermore, the focus on these “core” functions resulted in the exclusion of tissue microenvironmental effects on macrophage identity. It is now increasingly clear that macrophages have immense diversity in their origins and life spans and this diversity directly affects their function (Ginhoux *et al.*, 2010; Hoeffel and Ginhoux, 2015; van de Laar *et al.*, 2016). In addition to this, early myelopoietic processes which give rise to primitive macrophages precede most other tissue developmental processes. As a result, these macrophages enter into and reside in the rapidly changing developing tissue - pointing to possible roles during development. Mouse models were the ones first used to explore these developmental roles. However, two main problems serve to confound the results: firstly, the small numbers of rare cell types as well as the artefacts of the isolation protocol, and secondly, the significant differences between the brain development and organization of humans and mice. These factors have led to the emphasis on hiPSC - organoid models for the study of human tissue development. The CNS provides a fantastic system for the stepwise increase in complexity. The early emergence of the blood-brain barrier ends up isolating the CNS from the developmentally older more diverse cell types. This means that the development of the CNS as well as the role of microglia is much more robustly recapitulated in the *in vitro* organoid models. In this work, we attempted to develop an iPSC-derived organoid model which increased the complexity of the classical immuno-sufficient brain organoids established in our laboratory. We did this by integrating an iPSC-derived vascular network into the developing brain organoids, thereby generating a model with the capacity to demonstrate neuro-vascular-immune interactions.

4.1 Generation and co-culture of hiPSC-derived Brain Organoids

In this work, we decided to start with an attempt to replicate the brain organoid and iMac co-culture protocol previously established in the lab. In addition to the established protocol which is modified from the work by *Lancaster et al.*, we also generated brain organoids with a more cortical identity using the Dual-SMAD inhibition protocol described by *Sun et al.* (Lancaster and Knoblich, 2014; Sun *et al.*, 2022) Our goal at this stage was simple: ensure that we can consistently see the generation of the expected cell types and successfully replicate the changes in the organoid after co-culture previously seen in the lab. After ensuring successful ongoing differentiation by inspecting morphological features under a phase contrast microscope, we initiated co-culture of both protocols of brain organoids and observed the characteristic decrease in size after co-culture as well as signs of increased maturation in the brain organoids. This observation established our ability to exactly reproduce the current system studied in the lab - an essential requirement given the possibility of experimenter-specific variation while working with iPSCs. Once this requirement was met, we proceeded to establish a protocol for the generation of iPSC-derived blood vessels.

4.2 iPSC-derived Blood Vessel Organoids (BVOs)

This project was initially conceptualized on the initial work by Sun et al. who demonstrated the generation of ES cell-derived vascularized brain organoids by the fusion of two “vascular” organoids with one brain organoid in a matrigel droplet. Although their emphasis was on the characterization of the blood vessels as well as on the correction of the hypoxic environment in the core of the brain organoid, they also reported the generation of a large number of microglia. This immediately drew our interest as a strong candidate model for studying the immune involvement in neurodevelopmental as well as vasculogenic processes. First, however, we had to replicate their protocol and ensure it worked with our specific line of hiPSCs. hiPSCs are known for the possibility of “incomplete” induced pluripotency, where differences exist

between specific iPSC lines relating to their inherent propensity for certain differentiation trajectories.

We repeated each step of their protocol as is, including using media from the same supplier as well as analysis at identical time points using identical antibodies for flow cytometry. We also coupled this with regular light microscopy observation to look for signs of aberrant differentiation. However, despite our best attempts and multiple replicates, we were unable to reproduce their results. Their observation of almost 20% induction in endothelial cells was much higher than our ~1.5% induction of $CD31^+$ endothelial cells (Sun *et al.*, 2022). Furthermore, we were unable to detect any $CD14^+CD45^+$ double-positive cells further confirming the absence of microglia. We reasoned that the large number of undifferentiated cells would cause rogue interactions and preclude successful replication of our protocol. As a result, we decided to look for alternative protocols for the generation of iPSC-derived blood vessels.

We tried a large number of different protocols using different induction media as well as different concentrations of vasculogenic cytokines like VEGF and FGF-2. Furthermore, we also explored the use of small molecule patterning agents like Forskolin - a potent adenylyl cyclase activator. However, we were still unable to obtain >3% induction of endothelial cells. It was then we came across the seminal work by *Wimmer et al.* (Wimmer *et al.*, 2019b, 2019a; Nikolova *et al.*, 2022). What immediately caught our attention was the emphasis on the size of the blood vessel organoid and its impact on the efficiency of endothelial cell differentiation. Furthermore, this protocol focused on the generation of endothelial cells as well as pericytes which are not only essential constituents of the neurovascular unit but are also responsible for the survival of the endothelial cells and the stability of the blood vessel. We decided to attempt the generation of blood vessel organoids as described by Wimmer et al. but had to optimise the protocol for use in a 96-well plate in a manner similar to *Nikolova et al.* (Wimmer *et al.*, 2019b; Nikolova *et al.*, 2022). The latter modification was especially important owing to the use of flow cytometry for the measurement of cell proportions within the different fusion organoids. Interestingly, we were able to obtain much higher percentages of endothelial cell induction ~18% using this new protocol and decided to use it for the generation of vascularized brain organoids.

4.3 Development of a Protocol for the Vascularization of Brain Organoids

Once we had established the protocol for successful differentiation of blood vessel organoids, we decided to vascularize the brain organoid via fusion using co-embedding in matrigel - a modification of the approach discussed by *Sun et al*. (Sun *et al.*, 2022). However, in the quest for higher efficiency of blood vessel organoid differentiation, we had to reduce the size of the organoid to ~100µm at which size they were just barely visible. To get around this limitation, we had to develop a new workflow for embedding the blood vessel and brain organoid into one matrigel droplet while minimising blood vessel organoid loss. We also had to optimize the vasculogenic cytokine concentrations during organoid growth as well as co-culture which ensures maximum vessel sprouting while minimising off-target effects. Fourteen days after co-embedding, we were able to observe a close apposition between the blood vessels and CNS cell types in our fusion organoid as well as retention of the telltale morphological features associated with neurodevelopment. Furthermore, the co-culture of the fusion organoids with iMacs also revealed the characteristic decrease in size as well as an increased proportion of $CD31^+$ endothelial cells after co-culture.

4,4 The developmental role of Microglia and future directions

The involvement of microglia in the vascularization of the brain is a story of two unknowns. Not only is the possible mechanism of their interaction with growing blood vessels not known but also the existence of this interaction is itself an unresolved question. This problem then is very difficult to solve using classical genetic tools and mouse models. It does, however, represent an ideal case study for the use of single-cell transcriptomics as that would enable the identification of new microglial subtypes with an upregulated “vascular”/ “angiogenic” signature. This single-cell approach would also enable the identification of specific markers for these microglia and their spatial localization can then be determined using sectioning and confocal microscopy. The iPSC-organoid model with the previously discussed increase in complexity allows the

isolation of large numbers of iMicros which better covers the full range of microglial subsets - aiding the identification of a possible vasculogenic subset.

The possible role of microglia in the growth and maintenance of vasculature is not just based on the early microglial residence in the CNS. Primitive macrophages in the gut (of similar ontogeny to microglia) have shown roles in the maintenance of microvascular networks of the gut and neuroprotection (De Schepper *et al.*, 2018). Furthermore, macrophages under hypoxic conditions have shown the secretion of VEGF and promote of endothelial cell sprouting (Anandi *et al.*, 2023). Under adult brain conditions, astrocytes under hypoxia in close contact with blood vessels are the dominant sources of VEGF (Kaur *et al.*, 2006). This VEGF produced by astrocytes could promote angiogenic sprouting and expansion of the brain vasculature ((Tata *et al.*, 2015)However, astrocyte numbers increase predominantly during late neurodevelopment and I think in the early developing CNS, the microglia in a hypoxic environment could be responsible for this VEGF secretion thereby promoting the sprouting of the blood vessels.

The first step for future experiments would be a single-cell analysis and spatial-OMICS (to detect association with vessels). of the organoids to look for the emergence of new microglial subtypes which are different from those seen in non-vascularised co-cultured organoids. This will also help confirm the proper course of differentiation in the presence of high angiogenic cytokine concentrations. Further use of sectioning and immunohistochemistry will enable the identification of subtype-specific localizations of these microglia. To confirm the microglial involvement, depletion studies using CSF1R inhibitors can be used to further elaborate on the microglial role in the maintenance of the formed vascular network. Although the increased proportion of endothelial cells in Fig. 3.16b points to a possible vessel-promoting role of the microglia, we need to make a larger batch of organoids to ensure this effect isn't organoid-specific. Furthermore, the generation of brain and vessel organoids from untagged vs membrane-tagged fluorescent iPSC lines will enable easier identification of the source of the blood vessels enabling easier daily observation of ongoing differentiation. Lastly, and as a much longer-term goal, iPSC knockout lines of genes identified as being important in the preliminary screens can be used for in-depth mechanistic analysis of the role played by microglia during vascularization of the developing brain.

4.5 Limitations

It is important to understand that while the organoids represent a powerful system for the study of developmental processes, their existence *in vitro* and their inherent simplicity should add to the caution while interpreting the results. While I was unable to establish all the required controls due to time constraints, it is necessary to perform qPCR analysis on the various isolated and sorted cell types to ensure that the high cytokine amounts in the media do not fundamentally affect brain organoid differentiation. Moreover, a more precise gating strategy for endothelial cells needs to be designed as we did not have relevant positive controls to set the positive gate for the $CD31^{+}$ population. Furthermore, care must be taken while adapting these protocols to other ES/ iPS cell lines as significant variability can exist owing to “innate” differentiation trajectories. Lastly, attempts must always be made to explore this process in mice to ensure that the observed effect is not an artefact of the organoid model system.

5. References

Abud, EM et al. (2017). iPSC-Derived Human Microglia-like Cells to Study Neurological Diseases. Neuron 94, 278-293.e9.

Abutaleb, NO, and Truskey, GA (2021). Differentiation and characterization of human iPSC-derived vascular endothelial cells under physiological shear stress. STAR Protoc 2, 100394.

Allen, DE, Donohue, KC, Cadwell, CR, Shin, D, Keefe, MG, Sohal, VS, and Nowakowski, TJ (2022). Fate mapping of neural stem cell niches reveals distinct origins of human cortical astrocytes. Science 376, 1441–1446.

Anand, GM, Megale, HC, Murphy, SH, Weis, T, Lin, Z, He, Y, Wang, X, Liu, J, and Ramanathan, S (2023). Controlling organoid symmetry breaking uncovers an excitable system underlying human axial elongation. Cell 186, 497-512.e23.

Anandi, L, Garcia, J, Janská, L, Liu, J, Ros, M, and Carmona-Fontaine, C (2023). Direct visualization of emergent metastatic features within an *ex vivo* model of the tumor microenvironment, Cancer Biology.

Andrews, MG, Subramanian, L, Salma, J, and Kriegstein, AR (2022). How mechanisms of stem cell polarity shape the human cerebral cortex. Nat Rev Neurosci 23, 711–724.

Anthony, TE, Klein, C, Fishell, G, and Heintz, N (2004). Radial Glia Serve as Neuronal Progenitors in All Regions of the Central Nervous System. Neuron 41, 881–890.

Bain, G, Kitchens, D, Yao, M, Huettner, JE, and Gottlieb, DI (1995). Embryonic Stem Cells Express Neuronal Properties in Vitro. Dev Biol 168, 342–357.

Berghoff, SA et al. (2021). Microglia facilitate repair of demyelinated lesions via post-squalene sterol synthesis. Nat Neurosci 24, 47–60.

Bhaduri, A et al. (2020). Cell stress in cortical organoids impairs molecular subtype specification. Nature 578, 142–148.

Bowles, KR, T. C. W., J, Qian, L, Jadow, BM, and Goate, AM (2019). Reduced variability of neural progenitor cells and improved purity of neuronal cultures using magnetic activated cell sorting. PLoS ONE 14, e0213374.

Bruttger, J et al. (2015). Genetic Cell Ablation Reveals Clusters of Local Self-Renewing Microglia in the Mammalian Central Nervous System. Immunity 43, 92–106.

Chambers, SM, Fasano, CA, Papapetrou, EP, Tomishima, M, Sadelain, M, and Studer, L (2009). Highly efficient neural conversion of human ES and iPS cells by dual inhibition of SMAD signaling. Nat Biotechnol 27, 275–280.

De Schepper, S et al. (2018). Self-Maintaining Gut Macrophages Are Essential for Intestinal Homeostasis. Cell 175, 400-415.e13.

d'Errico, P et al. (2022). Microglia contribute to the propagation of Aβ into unaffected brain tissue. Nat Neurosci 25, 20–25.

Favuzzi, E et al. (2021). GABA-receptive microglia selectively sculpt developing inhibitory circuits. Cell 184, 4048-4063.e32.

Gadhoum, SZ, and Sackstein, R (2008). CD15 expression in human myeloid cell differentiation is regulated by sialidase activity. Nat Chem Biol 4, 751–757.

Geschwind, DH, and Rakic, P (2013). Cortical Evolution: Judge the Brain by Its Cover. Neuron 80, 633–647.

Giandomenico, SL, Sutcliffe, M, and Lancaster, MA (2021). Generation and long-term culture of advanced cerebral organoids for studying later stages of neural development. Nat Protoc 16, 579–602.

Ginhoux, F et al. (2010). Fate Mapping Analysis Reveals That Adult Microglia Derive from Primitive Macrophages. Science 330, 841–845.

Götz, M, and Huttner, WB (2005). The cell biology of neurogenesis. Nat Rev Mol Cell Biol 6, 777–788.

Grabert, K, Michoel, T, Karavolos, MH, Clohisey, S, Baillie, JK, Stevens, MP, Freeman, TC, Summers, KM, and McColl, BW (2016). Microglial brain region−dependent diversity and selective regional sensitivities to aging. Nat Neurosci 19, 504–516.

Guttikonda, SR et al. (2021). Fully defined human pluripotent stem cell-derived microglia and tri-culture system model C3 production in Alzheimer's disease. Nat Neurosci 24, 343–354.

Ham, O, Jin, YB, Kim, J, and Lee, M-O (2020). Blood vessel formation in cerebral organoids formed from human embryonic stem cells. Biochem Biophys Res Commun 521, 84–90.

Hamad, S, Derichsweiler, D, Gaspar, JA, Brockmeier, K, Hescheler, J, Sachinidis, A, and Pfannkuche, KP (2022). High-efficient serum-free differentiation of endothelial cells from human iPS cells. Stem Cell Res Ther 13, 251.

Hansen, DV, Lui, JH, Parker, PRL, and Kriegstein, AR (2010). Neurogenic radial glia in the outer subventricular zone of human neocortex. Nature 464, 554–561.

Hattori, Y, Naito, Y, Tsugawa, Y, Nonaka, S, Wake, H, Nagasawa, T, Kawaguchi, A, and Miyata, T (2020). Transient microglial absence assists postmigratory cortical neurons in proper differentiation. Nat Commun 11, 1631.

Hoeffel, G, and Ginhoux, F (2015). Ontogeny of Tissue-Resident Macrophages. Front Immunol 6.

Hong, S et al. (2016a). Complement and microglia mediate early synapse loss in Alzheimer mouse models. Science 352, 712–716.

Hong, S, Dissing-Olesen, L, and Stevens, B (2016b). New insights on the role of microglia in synaptic pruning in health and disease. Curr Opin Neurobiol 36, 128–134.

Huang, RD, Smith, MF, and Zahler, WL (1982). Inhibition of forskolin-activated adenylate cyclase by ethanol and other solvents. J Cyclic Nucleotide Res 8, 385–394.

Itskovitz-Eldor, J, Schuldiner, M, Karsenti, D, Eden, A, Yanuka, O, Amit, M, Soreq, H, and Benvenisty, N (2000). Differentiation of human embryonic stem cells into embryoid bodies compromising the three embryonic germ layers. Mol Med Camb Mass 6, 88–95.

Jiang, D, Burger, CA, Akhanov, V, Liang, JH, Mackin, RD, Albrecht, NE, Andrade, P, Schafer, DP, and Samuel, MA (2022). Neuronal signal-regulatory protein alpha drives microglial

phagocytosis by limiting microglial interaction with CD47 in the retina. Immunity 55, 2318-2335.e7.

Jordão, MJC et al. (2019). Single-cell profiling identifies myeloid cell subsets with distinct fates during neuroinflammation. Science 363, eaat7554.

Kaur, C, Sivakumar, V, Zhang, Y, and Ling, EA (2006). Hypoxia-induced astrocytic reaction and increased vascular permeability in the rat cerebellum. Glia 54, 826–839.

Kawasaki, H, Mizuseki, K, Nishikawa, S, Kaneko, S, Kuwana, Y, Nakanishi, S, Nishikawa, SI, and Sasai, Y (2000). Induction of midbrain dopaminergic neurons from ES cells by stromal cell-derived inducing activity. Neuron 28, 31–40.

Kierdorf, K et al. (2013). Microglia emerge from erythromyeloid precursors via Pu.1- and Irf8-dependent pathways. Nat Neurosci 16, 273–280.

Kosodo, Y, Suetsugu, T, Suda, M, Mimori-Kiyosue, Y, Toida, K, Baba, SA, Kimura, A, and Matsuzaki, F (2011). Regulation of interkinetic nuclear migration by cell cycle-coupled active and passive mechanisms in the developing brain. EMBO J 30, 1690–1704.

van de Laar, L et al. (2016). Yolk Sac Macrophages, Fetal Liver, and Adult Monocytes Can Colonize an Empty Niche and Develop into Functional Tissue-Resident Macrophages. Immunity 44, 755–768.

Lancaster, MA, and Knoblich, JA (2014). Generation of cerebral organoids from human pluripotent stem cells. Nat Protoc 9, 2329–2340.

Lancaster, MA, Renner, M, Martin, C-A, Wenzel, D, Bicknell, LS, Hurles, ME, Homfray, T, Penninger, JM, Jackson, AP, and Knoblich, JA (2013). Cerebral organoids model human brain development and microcephaly. Nature 501, 373–379.

Lehrman, EK et al. (2018). CD47 Protects Synapses from Excess Microglia-Mediated Pruning during Development. Neuron 100, 120-134.e6.

Liu, Y, Han, SSW, Wu, Y, Tuohy, TMF, Xue, H, Cai, J, Back, SA, Sherman, LS, Fischer, I, and Rao, MS (2004). CD44 expression identifies astrocyte-restricted precursor cells. Dev Biol 276, 31–46.

Malatesta, P, Hack, MA, Hartfuss, E, Kettenmann, H, Klinkert, W, Kirchhoff, F, and Götz, M (2003). Neuronal or Glial Progeny: Regional Differences in Radial Glia Fate. Neuron 37, 751–764.

Mansour, AA, Gonçalves, JT, Bloyd, CW, Li, H, Fernandes, S, Quang, D, Johnston, S, Parylak, SL, Jin, X, and Gage, FH (2018). An in vivo model of functional and vascularized human brain organoids. Nat Biotechnol 36, 432–441.

Marshall, JJ, and Mason, JO (2019). Mouse vs man: Organoid models of brain development & disease. Brain Res 1724, 146427.

Martynoga, B, Drechsel, D, and Guillemot, F (2012). Molecular Control of Neurogenesis: A View from the Mammalian Cerebral Cortex. Cold Spring Harb Perspect Biol 4, a008359.
Matcovitch-Natan, O et al. (2016). Microglia development follows a stepwise program to regulate brain homeostasis. Science 353, aad8670.

Möller, K, Brambach, M, Villani, A, Gallo, E, Gilmour, D, and Peri, F (2022). A role for the centrosome in regulating the rate of neuronal efferocytosis by microglia in vivo. ELife 11,

e82094.

Muffat, J et al. (2016). Efficient derivation of microglia-like cells from human pluripotent stem cells. Nat Med 22, 1358–1367.

Nakagawa, M, Koyanagi, M, Tanabe, K, Takahashi, K, Ichisaka, T, Aoi, T, Okita, K, Mochiduki, Y, Takizawa, N, and Yamanaka, S (2008). Generation of induced pluripotent stem cells without Myc from mouse and human fibroblasts. Nat Biotechnol 26, 101–106.

Nikolova, MT, He, Z, Wimmer, RA, Seimiya, M, Nikoloff, JM, Penninger, JM, Camp, JG, and Treutlein, B (2022). Fate and state transitions during human blood vessel organoid development, Developmental Biology.

Okita, K et al. (2011). A more efficient method to generate integration-free human iPS cells. Nat Methods 8, 409–412.

Okita, K, Nakagawa, M, Hyenjong, H, Ichisaka, T, and Yamanaka, S (2008). Generation of Mouse Induced Pluripotent Stem Cells Without Viral Vectors. Science 322, 949–953.
Ostrem, BEL, Lui, JH, Gertz, CC, and Kriegstein, AR (2014). Control of outer radial glial stem cell mitosis in the human brain. Cell Rep 8, 656–664.

Paolicelli, RC et al. (2011). Synaptic pruning by microglia is necessary for normal brain development. Science 333, 1456–1458.

Patsch, C et al. (2015). Generation of vascular endothelial and smooth muscle cells from human pluripotent stem cells. Nat Cell Biol 17, 994–1003.

Popova, G et al. (2021). Human microglia states are conserved across experimental models and regulate neural stem cell responses in chimeric organoids. Cell Stem Cell 28, 2153-2166.e6.

Qi, Y et al. (2017). Combined small-molecule inhibition accelerates the derivation of functional cortical neurons from human pluripotent stem cells. Nat Biotechnol 35, 154–163.

Qian, X et al. (2016). Brain-Region-Specific Organoids Using Mini-bioreactors for Modeling ZIKV Exposure. Cell 165, 1238–1254.

Rakic, P (2003). Elusive radial glial cells: Historical and evolutionary perspective. Glia 43, 19–32.

Rakic, P (2009). Evolution of the neocortex: a perspective from developmental biology. Nat Rev Neurosci 10, 724–735.

Ranawat, N, and Masai, I (2021). Mechanisms underlying microglial colonization of developing neural retina in zebrafish. ELife 10, e70550.

Rash, BG, Duque, A, Morozov, YM, Arellano, JI, Micali, N, and Rakic, P (2019). Gliogenesis in the outer subventricular zone promotes enlargement and gyrification of the primate cerebrum. Proc Natl Acad Sci U S A 116, 7089–7094.

Risau, W, and Wolburg, H (1990). Development of the blood-brain barrier. Trends Neurosci 13, 174–178.

Rosebrock, D et al. (2022). Enhanced cortical neural stem cell identity through short SMAD and WNT inhibition in human cerebral organoids facilitates emergence of outer radial glial cells. Nat Cell Biol 24, 981–995.

Roth, J, Brunel, L, Huang, M, Cai, B, Liu, Y, Sinha, S, Yang, F, Pasca, S, Shin, S, and Heilshorn, S (2023). Spatially controlled construction of assembloids using bioprinting, In Review.

Rymo, SF, Gerhardt, H, Wolfhagen Sand, F, Lang, R, Uv, A, and Betsholtz, C (2011). A two-way communication between microglial cells and angiogenic sprouts regulates angiogenesis in aortic ring cultures. PloS One 6, e15846.

Schafer, DP, Lehrman, EK, Kautzman, AG, Koyama, R, Mardinly, AR, Yamasaki, R, Ransohoff, RM, Greenberg, ME, Barres, BA, and Stevens, B (2012). Microglia Sculpt Postnatal Neural Circuits in an Activity and Complement-Dependent Manner. Neuron 74, 691–705.

Schulz, C et al. (2012). A Lineage of Myeloid Cells Independent of Myb and Hematopoietic Stem Cells. Science 336, 86–90.

Shemer, A et al. (2018). Engrafted parenchymal brain macrophages differ from microglia in transcriptome, chromatin landscape and response to challenge. Nat Commun 9, 5206.

Sidorov, MS, Kim, H, Rougie, M, Williams, B, Siegel, JJ, Gavornik, JP, and Philpot, BD (2020). Visual Sequences Drive Experience-Dependent Plasticity in Mouse Anterior Cingulate Cortex. Cell Rep 32, 108152.

Silva, CG, Peyre, E, and Nguyen, L (2019). Cell migration promotes dynamic cellular interactions to control cerebral cortex morphogenesis. Nat Rev Neurosci 20, 318–329.

Smith, AM, Gibbons, HM, Lill, C, Faull, RLM, and Dragunow, M (2013). Isolation and culture of adult human microglia within mixed glial cultures for functional experimentation and high-content analysis. Methods Mol Biol Clifton NJ 1041, 41–51.

Sturgeon, CM, Ditadi, A, Awong, G, Kennedy, M, and Keller, G (2014). Wnt signaling controls the specification of definitive and primitive hematopoiesis from human pluripotent stem cells. Nat Biotechnol 32, 554–561.

Subramanian, L, Bershteyn, M, Paredes, MF, and Kriegstein, AR (2017). Dynamic behaviour of human neuroepithelial cells in the developing forebrain. Nat Commun 8, 14167.

Sun, X-Y, Ju, X-C, Li, Y, Zeng, P-M, Wu, J, Zhou, Y-Y, Shen, L-B, Dong, J, Chen, Y-J, and Luo, Z-G (2022). Generation of vascularized brain organoids to study neurovascular interactions. ELife 11, e76707.

Takahashi, K, Tanabe, K, Ohnuki, M, Narita, M, Ichisaka, T, Tomoda, K, and Yamanaka, S (2007). Induction of Pluripotent Stem Cells from Adult Human Fibroblasts by Defined Factors. Cell 131, 861–872.

Takahashi, K, and Yamanaka, S (2006). Induction of Pluripotent Stem Cells from Mouse Embryonic and Adult Fibroblast Cultures by Defined Factors. Cell 126, 663–676.

Takahashi, T, Nowakowski, RS, and Caviness, VS (1993). Cell cycle parameters and patterns of nuclear movement in the neocortical proliferative zone of the fetal mouse. J Neurosci 13, 820–833.

Takata, K et al. (2017). Induced-Pluripotent-Stem-Cell-Derived Primitive Macrophages Provide a Platform for Modeling Tissue-Resident Macrophage Differentiation and Function. Immunity 47, 183-198.e6.

Takebe, T, Zhang, R-R, Koike, H, Kimura, M, Yoshizawa, E, Enomura, M, Koike, N, Sekine, K,

and Taniguchi, H (2014). Generation of a vascularized and functional human liver from an iPSC-derived organ bud transplant. Nat Protoc 9, 396–409.

Tata, M, Ruhrberg, C, and Fantin, A (2015). Vascularisation of the central nervous system. Mech Dev 138, 26–36.

Thomson, JA, Itskovitz-Eldor, J, Shapiro, SS, Waknitz, MA, Swiergiel, JJ, Marshall, VS, and Jones, JM (1998). Embryonic stem cell lines derived from human blastocysts. Science 282, 1145–1147.

Venegas, C et al. (2017). Microglia-derived ASC specks cross-seed amyloid-β in Alzheimer's disease. Nature 552, 355–361.

Wimmer, RA et al. (2019a). Human blood vessel organoids as a model of diabetic vasculopathy. Nature 565, 505–510.

Wimmer, RA, Leopoldi, A, Aichinger, M, Kerjaschki, D, and Penninger, JM (2019b). Generation of blood vessel organoids from human pluripotent stem cells. Nat Protoc 14, 3082–3100.

Xia, X, and Zhang, S-C (2009). Differentiation of neuroepithelia from human embryonic stem cells. Methods Mol Biol Clifton NJ 549, 51–58.

Zhang, SC, Wernig, M, Duncan, ID, Brüstle, O, and Thomson, JA (2001). In vitro differentiation of transplantable neural precursors from human embryonic stem cells. Nat Biotechnol 19, 1129–1133.

Zhao, Z et al. (2022). Organoids. Nat Rev Methods Primer 2, 1–21.

Zhu, Z, and Huangfu, D (2013). Human pluripotent stem cells: an emerging model in developmental biology. Dev Camb Engl 140, 705–717.